

# 000 001 002 003 004 005 FRAMEORACLE: LEARNING WHAT TO SEE AND HOW 006 MUCH TO SEE IN VIDEOS 007 008 009

010 **Anonymous authors**  
011 Paper under double-blind review  
012  
013  
014  
015  
016  
017  
018  
019  
020  
021  
022  
023  
024  
025  
026

## ABSTRACT

027 Vision-language models (VLMs) have advanced video understanding, but their  
028 performance is limited by the number of input frames they can process. Existing  
029 frame sampling strategies, such as uniform or fixed-budget selection, often  
030 fail to adapt to variations in information density or task complexity, resulting in  
031 inefficiency and information loss. To address this, we present **FrameOracle**, a  
032 lightweight and plug-and-play module that predicts both (1) which frames are  
033 most relevant to a given query and (2) how many frames are needed. FrameOracle  
034 is trained using a four-stage curriculum, with the first three stages relying  
035 on weak proxy signals such as cross-modal similarity. In the final stage, it lever-  
036 ages stronger supervision from a new dataset we introduce, **FrameOracle-41K**,  
037 the first large-scale VideoQA collection to provide keyframe annotations spec-  
038 ifying the minimal set of frames required to answer each question. Extensive  
039 experiments across five VLMs and six benchmarks demonstrate that FrameOracle  
040 reduces 16-frame inputs to an average of 10.4 frames without any loss in accuracy.  
041 When starting from 64-frame candidates, it reduces the input to an average of 13.9  
042 frames while improving accuracy by 1.4%, achieving state-of-the-art efficiency-  
043 accuracy trade-offs for scalable video understanding.  
044

## 1 INTRODUCTION

045 Rapid advances in large language models (LLMs) (Stiennon et al., 2020; Gao et al., 2022; Yang et al.,  
046 2024) have enabled vision-language models (VLMs) to integrate visual understanding with strong  
047 linguistic reasoning (Zhang et al., 2024; Bai et al., 2025; Zhang et al., 2025a). This makes VLMs  
048 highly effective for complex video tasks such as question answering (Zhang et al., 2023; Lin et al.,  
049 2024a;b; Zhao et al., 2024; Xiao et al., 2025), summarization (Hua et al., 2025; Lee et al., 2025),  
050 and instruction following (Ren et al., 2024; Qian et al., 2024). A key challenge, however, is the  
051 large volume of data these models must process. Processing every video frame is computationally  
052 expensive, making efficient frame sampling essential (Hu et al., 2025). Most VLMs currently rely  
053 on simple approaches, such as uniform sampling at a fixed frame rate or selecting a fixed number  
054 of frames. While easy to implement, these methods have clear drawbacks: in long videos, they may  
055 miss crucial information, whereas in short videos, they often introduce redundant frames that waste  
056 resources, distract the model, and obscure key moments.  
057

058 To mitigate this, a growing body of work has explored keyframe selection methods (Liu et al., 2025;  
059 Park et al., 2024; Tang et al., 2025; Zhang et al., 2025d). These approaches aim to identify a sub-  
060 set of frames that preserves semantic content while reducing redundancy. However, most existing  
061 methods assume a fixed, preset number of keyframes, ignoring the fact that the optimal number of  
062 frames varies across videos and queries. For example, short action-centric questions (e.g., whether a  
063 ball crosses a line in sports footage) may be resolved with just a handful of frames, while long-form  
064 narrative reasoning (e.g., inferring character intentions in a film) often requires a substantially larger  
065 set of frames. A few recent methods enable adaptive frame selection, but their adaptivity remains  
066 limited. In some cases, the selector is trained jointly with the backbone VLM (Buch et al., 2025),  
067 making it non-transferable to other models. In others, adaptivity is achieved via threshold-based  
068 filtering at inference, retaining only keyframes above a preset reward threshold. While this produces  
069 variable frame counts, it is not explicitly optimized during training, reducing effectiveness and gen-  
070 eralizability. This raises a fundamental question: *How can we design a selector that identifies the*

054 *most relevant frames for a given query and determines how many are needed, while generalizing*  
 055 *across different VLMs?*

056 To this end, we propose **FrameOracle**, a lightweight, plug-and-play frame selector that can be in-  
 057 tegrated with arbitrary VLMs. Unlike prior approaches that fix the number of frames in advance  
 058 or require co-training with a specific backbone, FrameOracle jointly predicts (1) the importance of  
 059 each frame relative to the query and (2) the number of frames to retain. The module is trained with  
 060 a four-stage curriculum. The first three stages rely on weak proxy signals, such as cross-modal  
 061 similarity and leave-one-out loss degradation. The final stage leverages stronger supervision from  
 062 a new dataset we create, **FrameOracle-41K**, a large-scale VideoQA dataset with 40,992 examples  
 063 and the first to provide keyframe annotations specifying the minimal frames required to answer each  
 064 question. Unlike tasks such as object detection (Lin et al., 2014) or captioning (Xiong et al., 2024),  
 065 no existing dataset provides ground-truth annotations identifying the keyframes. FrameOracle dy-  
 066 mically adapts its selections based on both video content and the prompt, operating seamlessly as  
 067 a pre-processing module for any downstream VLM. In summary, our contributions are as follows:

- 068 • We propose **FrameOracle**, a lightweight and plug-and-play frame selector that dynami-  
 069 cally predicts both which frames are most relevant and how many are needed.
- 070
- 071 • To facilitate training, we introduce **FrameOracle-41K**, the first large-scale VideoQA  
 072 dataset with keyframe annotations, specifying the minimal set of frames needed to answer  
 073 each question.
- 074
- 075 • We conduct extensive experiments across five VLMs and six benchmarks, showing that  
 076 FrameOracle reduces 16-frame inputs to an average of 10.4 frames without any loss in ac-  
 077 curacy. When starting from 64-frame candidates, it reduces the input to an average of 13.9  
 078 frames while improving accuracy by 1.4%, achieving state-of-the-art efficiency-accuracy  
 079 trade-offs for video understanding.

## 082 2 RELATED WORK

083 **Keyframe Selection for Video Understanding.** Most existing keyframe selection methods assume  
 084 a fixed frame budget: they rank candidate frames by visual-linguistic relevance or temporal salience  
 085 and then retain the top- $k$  subset (Liang et al., 2024; Tan et al., 2024; Yu et al., 2025; Liu et al.,  
 086 2025; Fang et al., 2025; Tang et al., 2025). Beyond this fixed-budget paradigm, some work has ex-  
 087 plored adaptive frame selection. These approaches fall into two categories. The first are agent-based  
 088 methods, where large multimodal models act as decision-makers that iteratively analyze videos. For  
 089 instance, VCA (Yang et al., 2025) combines curiosity-driven exploration with tree search to identify  
 090 informative segments, while AKeyS (Fan et al., 2025) leverages a language agent to heuristically  
 091 expand video segments and decide both which frames to retain and when to stop. However, such  
 092 methods are computationally expensive due to repeated agent calls. The second category comprises  
 093 approaches that require co-training with a specific VLM backbone (Buch et al., 2025; Yu et al., 2023;  
 094 Guo et al., 2025), which restricts their portability. In contrast, FrameOracle is adaptive, lightweight,  
 095 and model-agnostic: it learns to jointly predict which frames are relevant and how many to retain,  
 096 while remaining plug-and-play across diverse VLMs.

097 **Datasets and Supervision for Video-Language Models.** Progress in video-language reason-  
 098 ing has been driven by large-scale datasets such as LLaVA-Video-178K (Zhang et al., 2024),  
 099 ShareGPT4Video (Chen et al., 2024b), VideoRefer (Yuan et al., 2025), and CinePile (Rawal et al.,  
 100 2024), which cover diverse scenarios and support both short- and long-form understanding. How-  
 101 ever, most of these datasets provide supervision only at the answer level, leaving the underlying  
 102 evidence unannotated. In the absence of frame-level labels, keyframe selection methods are typ-  
 103 ically forced to rely on proxy signals, such as leave-one-out degradation or heuristic scoring. A  
 104 few benchmarks, such as TVQA+ (Lei et al., 2020), ReXTime (Chen et al., 2024a), and HourVideo  
 105 (Chandrasegaran et al., 2024), move toward span-level annotations, but none supply labels for both  
 106 the indices of keyframes and the minimal sufficient number of frames needed to answer a question.  
 107 FrameOracle-41K is the first dataset to provide explicit keyframe annotations for video-question  
 pairs, offering high-quality supervision for both training and evaluation of adaptive frame selectors.

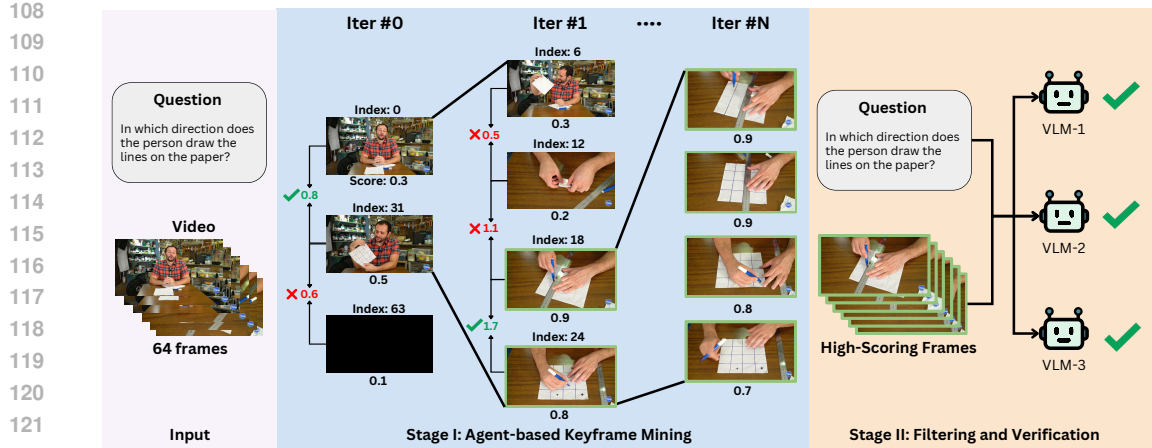


Figure 1: **FrameOracle-41K data generation pipeline.** Stage I (agent-based keyframe mining) iteratively explores each video using a multimodal agent, ultimately returning a predicted answer with confidence and relevance scores for all visited frames. Stage II (filtering and verification) first discards frames with low relevance scores and then verifies sufficiency by requiring three independent VLMs to answer correctly using only the remaining keyframes.

### 3 FRAMEORACLE-41K DATASET

We introduce FrameOracle-41K, the first VideoQA dataset that provides keyframe annotations, specifying the minimal set of frames needed to answer each question. The corpus contains 40,992 video–question pairs spanning diverse scenes and durations. In contrast to existing VideoQA datasets, which provide only ground-truth answers and, in some cases, coarse temporal spans in the video, FrameOracle-41K records, for each instance, the minimal number of frames needed to answer the question with high confidence, along with the keyframes that constitute the necessary evidence. Below, we describe our data generation pipeline, the verification and filtering procedures used to retain high-quality data, and the key statistics of the dataset.

#### 3.1 DATA GATHERING AND PROCESSING

All video–question pairs in FrameOracle-41K are sourced from LLaVA-Video-178K (Zhang et al., 2024), a large-scale VideoQA dataset that covers a wide range of scenarios and activities. From this corpus, we first select nearly 100K videos, each 2–3 minutes long, balancing adequate temporal context with a manageable annotation effort. We then apply a two-stage process to create the final dataset (Figure 1). *Stage I (agent-based keyframe mining)* automatically extracts candidate keyframes using a multimodal agent that iteratively explores each video and assigns frame-level relevance scores. *Stage II (filtering and verification)* selects the minimal sufficient frame subset by retaining only samples where three independent VLMs consistently answer the question correctly. We further conduct a human verification on 4,000 randomly sampled instances, achieving an inter-annotator agreement of 94% and a verified accuracy of 93.3%. This confirms the reliability of the automatically generated annotations. Detailed procedures for each stage are described in the following paragraphs. Example JSON entries are in Appendix B, human verification protocol and results in Appendix E, and dataset visualizations in Appendix H.

**Stage I: Agent-based Keyframe Mining.** Starting from a uniformly sampled set of 64 frames, we employ an agent built on Qwen2.5-VL-72B API (Bai et al., 2025) to iteratively explore the video with respect to the given question. In the first iteration, the agent inspects three anchor frames (indices 0, 31, and 63), assigns relevance scores, and attempts an answer with a confidence estimate. It then compares the pairwise summed relevance of adjacent anchors (0+31 vs. 31+63) to decide which segment to explore next. Within the selected segment, a denser set of four anchor frames is sampled, another answer with confidence is attempted, and the same pairwise relevance comparison guides subsequent iterations. This iterative score–refine cycle continues until either the agent becomes confident enough to provide a stable answer or all frames have been examined. By the end of Stage I, the agent returns (1) its predicted answer and confidence, and (2) the complete set of

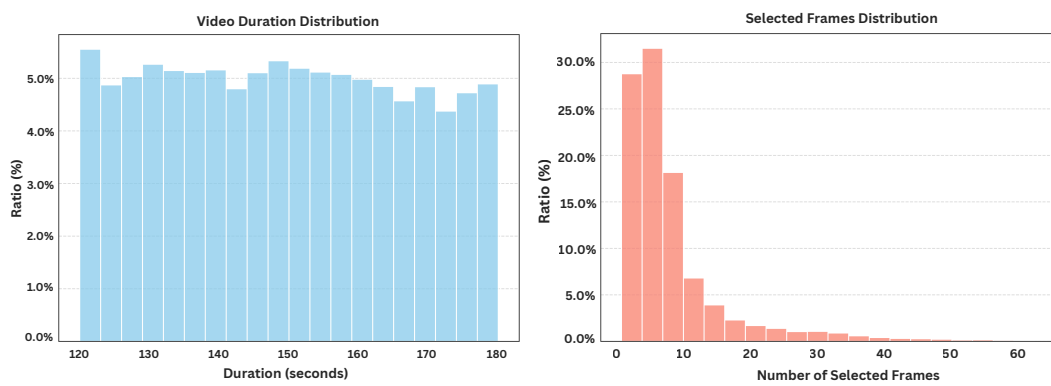


Figure 2: **FrameOracle-41K video-level statistics.** **Left:** Distribution of video durations. **Right:** Distribution of minimal sufficient keyframes per video–question pair.

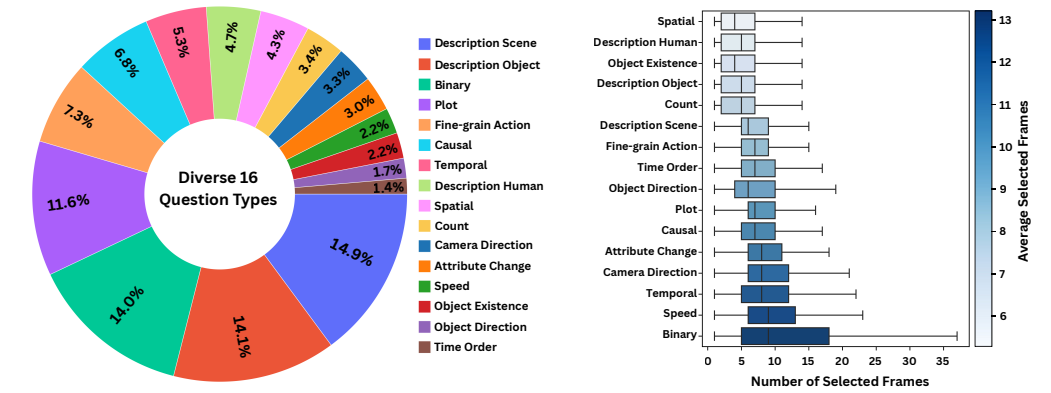


Figure 3: **FrameOracle-41K question-level statistics.** **Left:** Distribution of 16 question types across the dataset. **Right:** Per-type distributions of minimal sufficient keyframes.

frames it has inspected, each annotated with a relevance score. Any video–question pair for which the agent’s predicted answer does not match the ground-truth answer is then discarded. This mined trajectory captures both the localization of question-specific evidence and fine-grained frame-level importance signals, forming the raw candidates for the next stage.

**Stage II: Filtering and Verification.** After obtaining candidate keyframes from Stage I, we first remove all frames with relevance scores below a threshold  $\lambda$ , leaving only those with stronger relevance. For each video–question pair, we then test whether the selected keyframes alone are sufficient to answer the question. Specifically, the keyframe set and the question are fed into three independent VLMs (i.e., Qwen2.5-VL-72B (Bai et al., 2025), LLaVA-OneVision-72B (Li et al., 2025), and LLaVA-Video-72B (Zhang et al., 2024)), and their predictions are compared against the ground-truth answer. Only instances for which all three models succeed using only the keyframes are retained. This cross-model verification ensures that the released dataset contains consistent, question-grounded keyframe annotations.

### 3.2 DATASET STATISTICS

Our two-stage pipeline produces 40,992 video–question pairs, forming the FrameOracle-41K dataset. Figure 2 (left) shows that most videos are two to three minutes long, providing sufficient temporal context without excessive redundancy. Figure 2 (right) shows the distribution of minimal sufficient keyframes per video–question pair: the median is five frames, the mean is around seven, and over 80% of samples require no more than 10 frames. A small fraction of more complex cases need 30 or more frames.

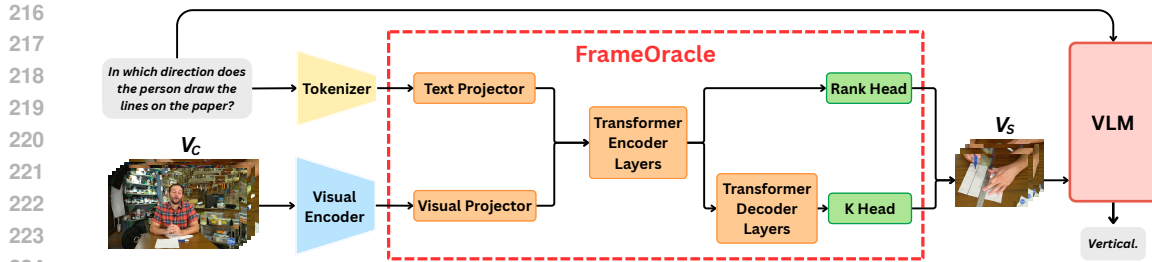


Figure 4: **Overview of the FrameOracle pipeline.** FrameOracle (dashed box) receives raw video frames and the textual prompt, and jointly predicts frame importance and the number of frames to keep. It outputs a compact keyframe subset, which is fed into the downstream VLM.  $V_C$  denotes the pre-sampled frame collection, and  $V_S$  denotes the subset selected by FrameOracle.

Figure 3 (left) categorizes all questions into 16 types following the taxonomy introduced in LLaVA-Video-178K (Zhang et al., 2024), covering a broad spectrum of reasoning skills such as description, localization, temporal understanding, and causal inference. Figure 3 (right) shows the per-type distribution of minimal keyframes. *Spatial* questions require the fewest frames (about 5.3 frames), while *Binary* questions need the most (around 13 frames), reflecting their underlying evidence needs. *Spatial* questions focus on static layouts within a scene, whereas *Binary* questions often ask whether an event occurs at any moment, requiring inspection of a broader temporal range. Some categories, such as *Camera Direction*, *Temporal*, *Speed*, and *Binary*, show high intra-class variability, with the number of required frames varying widely across instances. This indicates that even within a single reasoning type, temporal complexity and evidence density can differ significantly, highlighting the heterogeneous nature of FrameOracle-41K and motivating adaptive frame selection. Complete dataset statistics, question type definitions, and textual analyses are provided in Appendix D.

## 4 METHOD

We introduce **FrameOracle**, a lightweight and adaptive frame selector that dynamically determines the appropriate number of keyframes from a video, conditioned on the user prompt. FrameOracle enables efficient video understanding by providing the downstream VLM with a compact yet highly relevant subset of frames.

Since directly processing all frames of a video,  $V$ , is computationally expensive, we first apply uniform temporal sampling to extract a candidate set of  $N$  frames, denoted as  $V_C = \{f_1, \dots, f_N\}$ . This pre-sampling step acts as a coarse filter, reducing the input to a manageable size for FrameOracle (e.g.,  $N = 64$  or  $N = 16$ ). Our goal is to learn FrameOracle, a *selection policy*,  $\Pi_\theta$ , parameterized by  $\theta$ , that operates on the candidate set. Given a candidate set  $V_C$  and a text prompt  $P$ , FrameOracle selects a compact subset of frames  $V_S \subset V_C$ . Unlike approaches that fix the number of selected frames in advance, FrameOracle dynamically determines the subset size,  $K = |V_S|$ , as part of the selection process. Formally,  $\Pi_\theta$  maps the pair  $(V_C, P)$  to the selected subset  $V_S$ , which is then passed to a downstream VLM,  $\mathcal{M}$ , to perform a reasoning task, producing an output  $A = \mathcal{M}(V_S, P)$ . The objective is to train  $\Pi_\theta$  to choose subsets that maximize the performance of  $\mathcal{M}$  while keeping  $K$  as small as possible.

### 4.1 FRAMEORACLE

FrameOracle,  $\Pi_\theta$ , is a neural module that learns to jointly predict frame importance and the number of frames to select from the candidate set  $V_C$ . We begin by extracting features from both the video frames and the text prompt, which serve as inputs to FrameOracle. For the candidate frame set  $V_C$ , we use a visual encoder to generate a sequence of  $N$  frame embeddings. The text prompt  $P$  is encoded using a tokenizer to obtain text embeddings. FrameOracle then operates on the projected embeddings and is fully agnostic to the underlying tokenizer. The FrameOracle architecture, shown in Figure 4, is composed of two main components: (1) a cross-modal fusion encoder and (2) dual prediction heads.

270     **(1) Cross-Modal Fusion.** To model the relationship between the text query and the video, we  
 271     fuse the two modalities. Frame and text embeddings are first projected into a shared latent space  
 272     using linear layers, and then processed by a stack of Transformer encoder layers. Specifically, we  
 273     concatenate the projected text and frame embeddings, together with a learnable query token, into  
 274     a single sequence  $[k_{\text{query}}; \text{text}; \text{frames}]$ , which is processed by the encoder whose self-attention  
 275     performs token-level cross-modal interaction. Each frame is represented by one frame-level token,  
 276     enabling efficient reasoning across text and frames with negligible computational cost relative to the  
 277     downstream VLM.

278     **(2) Dual Prediction Heads.** The output of the fusion encoder is passed to two specialized heads,  
 279     which form the core of our selection policy:

- 281     • **Rank Head:** This head evaluates the relevance of each candidate frame to the prompt. It  
 282     processes the fused feature sequence to output a scalar importance score,  $s_i$ , for each frame  
 283      $f_i \in V_C$ , resulting in a score vector  $S = \{s_1, \dots, s_N\}$ .
- 284     • **K Head:** This head predicts how many frames to select from the candidate set. It takes the  
 285     globally aggregated features from the fusion encoder and outputs a probability distribution  
 286     over a discrete set of possible values for  $K$ , where  $K \leq N$ .

## 288     4.2 TRAINING

290     We train FrameOracle using a curriculum-based, four-stage protocol. This strategy progressively  
 291     refines the policy  $\Pi_\theta$ , teaching it to reason effectively over the pre-sampled frames (e.g., 16 or 64).  
 292     The staged training leverages four widely used public VideoQA datasets, covering clips ranging  
 293     from roughly 10 seconds to 15 minutes in length. Details of the full dataset composition are provided  
 294     in Appendix A.

295     **Stage 1: Text-Visual Alignment.** The initial stage focuses on learning a robust cross-modal rep-  
 296     resentation by aligning the textual prompt with the visual content of the candidate frames. We use  
 297     the pre-trained text-visual model SigLIP (Zhai et al., 2023) as a teacher to provide supervision. For  
 298     each prompt-frame pair, a SigLIP similarity score serves as the target relevance signal. The feature  
 299     projectors and the cross-modal Transformer encoder are trained with a RankNet loss (Burges et al.,  
 300     2005), encouraging the model’s predicted scores to match the relative ordering of the SigLIP simi-  
 301     larities. Concretely, for any two frames  $i$  and  $j$ , let  $s_i$  and  $s_j$  denote their SigLIP similarity scores,  
 302     and  $y_i$  and  $y_j$  their predicted scores. We define the pairwise preference label as  $t_{ij} = \text{sign}(s_i - s_j)$ .  
 303     The RankNet loss is then given by

$$304 \quad \mathcal{L}_{\text{RankNet}} = \sum_{i < j} \log \left( 1 + \exp \left( -t_{ij} (y_i - y_j) \right) \right), \quad (1)$$

307     where  $t_{ij} = 0$  corresponds to tied frames and does not contribute to the gradient. In this way, the  
 308     alignment capability of SigLIP is distilled into FrameOracle. The K Head remains frozen during  
 309     this stage.

310     **Stage 2: Rank Head Optimization.** In the second stage, we train the Rank Head to identify the  
 311     most salient frames in the candidate set  $V_C$ . Unlike the first stage, where SigLIP-based supervision  
 312     is computed independently for each frame and provides no temporal guidance, this stage uses the  
 313     downstream VLM’s loss as a supervisory signal, allowing the selector to capture temporal depen-  
 314     dencies across frames. To generate training targets, we adopt a leave-one-out (LOO) approach: for  
 315     each frame  $f_i \in V_C$ , we remove it from the input set and pass the remaining frames through the  
 316     VLM, measuring the change in its loss. A larger increase indicates that  $f_i$  is more important. These  
 317     importance scores serve as soft targets, and the Rank Head is trained with a RankNet loss to predict  
 318     them. During this stage, the K Head remains frozen, while the Transformer encoder and feature  
 319     projectors are fine-tuned with a smaller learning rate to stabilize training.

320     **Stage 3: K Head Optimization.** The third stage focuses on training the K Head to predict the  
 321     number of frames. During this stage, the Rank Head is frozen, while the feature projectors and the  
 322     Transformer encoder are fine-tuned with a very small learning rate for slight adaptation. For each  
 323     sample, we evaluate the downstream VLM (the same backbone and task loss as in Stage 2) using  
 324     the top- $k$  frames from  $V_C$ , ranked by the frozen Rank Head, for a candidate value  $k \in N$ . We then

324 select the target

325 
$$k^* = \arg \min_{k \in N} \left( \text{zscore}(\mathcal{L}_{\text{task}}(k)) + \lambda_k k \right), \quad (2)$$

327 where the linear penalty balances accuracy and frame cost. The K Head predicts a categorical  
328 distribution  $p_{\theta}(k)$  over  $k \in \{1, \dots, N\}$  and is trained with

329 
$$\mathcal{L}_K = (1 - \alpha) \mathcal{L}_{\text{evo}} + \alpha \mathcal{L}_{\text{class}}, \quad (3)$$

331 where the Expected Value Objective

332 
$$\mathcal{L}_{\text{evo}} = \text{SmoothL1} \left( \sum_{k=1}^N k p_{\theta}(k), k^* \right)$$

335 regresses the predicted expectation to  $k^*$ , and  $\mathcal{L}_{\text{class}}$  is a KL divergence aligning  $p_{\theta}$  with a Gaussian-  
336 shaped soft target centered at  $k^*$ .  
337338 **Stage 4: Supervised Fine-tuning with Ground Truth.** In the final stage, we perform super-  
339 viewed fine-tuning (SFT) on FrameOracle-41K, which provides supervision for both the keyframe  
340 indices and the number of frames. Unlike the earlier stages, which rely on weak or proxy signals,  
341 FrameOracle-41K offers high-quality annotations that have been verified for consistency. The Rank  
342 Head is trained to align its predictions with the annotated keyframes, while the K Head is jointly  
343 trained to match the annotated  $K$  values. This strong, direct supervision further refines the selection  
344 policy beyond what is achieved in Stages 1–3.345 

## 5 EXPERIMENTS

346 

### 5.1 EXPERIMENT SETTINGS

347 **Implementation Details.** We train two versions of FrameOracle, using uniformly sampled frames  
348 as selector inputs: one with 16 frames and another with 64 frames, respectively. Both of them use  
349 DINOv2 (Oquab et al., 2024) as the visual encoder and Qwen2.5-VL as the tokenizer. Training  
350 follows the four-stage curriculum described in Section 4.2, progressively optimizing the Rank Head  
351 and K Head using proxy signals and FrameOracle-41K annotations. In Stages 2 and 3, we adopt  
352 Qwen2.5-VL-3B as the backbone VLM for supervision. For the 64-frame selector, we additionally  
353 cap the maximum predicted  $K$  at 16 during Stage 3 to ensure comparability with the experimental  
354 settings. All experiments are run on 8×H100 GPUs. Detailed hyperparameter settings, including  
355 learning rates, batch sizes, and training durations for each stage, are provided in Appendix A.356 **Benchmarks.** We evaluate FrameOracle on six widely adopted video benchmarks, which can be  
357 divided into long-video and short-video understanding tasks. For long-video understanding, we in-  
358 clude EgoSchema (Mangalam et al., 2023), LongVideoBench (Wu et al., 2024), MLVU (Zhou et al.,  
359 2025), and Video-MME (Fu et al., 2025), all of which require reasoning over extended temporal  
360 contexts ranging from minutes to hours. These datasets emphasize challenges such as cross-event  
361 reasoning, global consistency, and temporal grounding across lengthy sequences. For short-video  
362 understanding, we evaluate on NExTQA (Xiao et al., 2021), and Perception (Pătrăucean et al., 2023),  
363 which involve clips typically within tens of seconds. These benchmarks focus on fine-grained event  
364 recognition, local temporal relations, and reasoning within concise videos. We follow the LMMs-  
365 Eval library (Zhang et al., 2025b) for evaluation, and report accuracy across all benchmarks.  
366367 

### 5.2 RESULTS AND ANALYSIS

368 **Comparisons with State-of-the-Art Models.** Table 1 presents a comprehensive comparison of  
369 FrameOracle across two categories: (1) **five** state-of-the-art (SOTA) VLMs, and (2) its integra-  
370 tion with six diverse VLMs, Qwen2.5-VL (Bai et al., 2025), LLaVA-OneVision (Li et al., 2025),  
371 LLaVA-Video (Zhang et al., 2024), VideoLLaMA3 (Zhang et al., 2025a), **Qwen3-VL(QwenTeam,**  
372 **2025**), and the proprietary GPT-4o (Hurst et al., 2024). **Qwen-VL series** internally merges every  
373 two adjacent frames into a single representation. To ensure a fair comparison with models that pro-  
374 cess raw frames directly, we report the baseline using 32 frames. For each model integrated with  
375 FrameOracle, we report results for two configurations: using 16-frame FrameOracle and 64-frame  
376 FrameOracle.  
377

378 Table 1: **FrameOracle vs. SOTA VLMs.** ‘‘Frames’’ shows  $M \rightarrow \bar{K}$ : FrameOracle starts from  $M$   
379 uniformly sampled frames and reduces to an average of  $\bar{K}$ . Highlighted rows show the upper-bound  
380 performance with larger frame inputs. LVB = LongVideoBench validation set.

Model	Frames	NExTQA			Perception	LVB	Video-MME	EgoSchema	MLVU	Avg.
		OE_val	OE_test	MC						
<i>(1) State-of-the-Art Models</i>										
ShareGPT4Video-8B (Chen et al., 2024b)	16	-	-	-	-	41.8	39.9	-	46.4	-
LLaMA-VID-7B (Li et al., 2024b)	16	-	-	-	44.6	-	25.9	38.5	33.2	-
VideoChat2-7B (Li et al., 2024a)	16	-	-	-	-	39.3	39.5	63.6	44.5	-
VideoLLaMA2-7B (Cheng et al., 2024)	16	-	-	45.4	54.9	53.1	47.9	53.1	-	-
InternVL2-40B (OpenGVLab, 2024)	16	-	-	-	-	59.3	61.2	-	59.5	-
<i>(2) FrameOracle on Different Baselines</i>										
Qwen2.5-VL-3B (Bai et al., 2025)	32	25.1	29.6	75.4	65.9	54.1	58.4	53.4	59.4	52.7
+ FrameOracle	32→20.9	25.6	30.5	74.8	66.7	54.3	58.5	53.8	58.4	52.8
+ FrameOracle	128→27.8	<b>26.0</b>	<b>31.7</b>	<b>76.1</b>	<b>67.8</b>	<b>54.8</b>	<b>59.7</b>	<b>54.5</b>	<b>61.6</b>	<b>54.0</b>
LLaVA-OneVision-7B (Li et al., 2025)	16	14.6	16.7	78.2	56.4	55.0	56.1	60.8	60.9	49.8
+ FrameOracle	16→10.4	16.1	17.8	77.6	56.5	55.5	56.0	62.4	60.2	50.3
+ FrameOracle	64→13.9	<b>16.5</b>	<b>19.0</b>	<b>78.5</b>	<b>56.9</b>	<b>56.5</b>	<b>58.1</b>	<b>63.4</b>	<b>63.7</b>	<b>51.6</b>
LLaVA-Video-7B (Zhang et al., 2024)	16	27.3	32.4	81.0	64.3	55.8	59.8	54.2	61.7	54.6
+ FrameOracle	16→10.4	27.8	33.0	80.4	64.7	56.3	59.6	54.6	60.8	54.7
+ FrameOracle	64→13.9	<b>28.8</b>	<b>33.9</b>	<b>81.6</b>	<b>65.1</b>	<b>57.8</b>	<b>61.6</b>	<b>55.2</b>	<b>64.3</b>	<b>56.0</b>
VideoLLaMA3-7B (Zhang et al., 2025a)	16	27.8	32.3	<b>82.3</b>	72.3	56.1	61.2	61.4	50.9	55.5
+ FrameOracle	16→10.4	28.3	32.9	81.2	72.0	56.0	61.4	61.8	52.8	55.8
+ FrameOracle	64→13.9	<b>28.9</b>	<b>33.6</b>	82.0	<b>72.8</b>	<b>56.9</b>	<b>61.8</b>	<b>62.4</b>	<b>54.1</b>	<b>56.6</b>
Qwen3-VL-3B (QwenTeam, 2025)	32	26.0	31.1	76.6	67.5	63.3	66.9	70.8	63.6	58.2
+ FrameOracle	32→20.9	26.6	32.3	76.1	68.2	64.0	67.3	71.4	62.9	58.6
+ FrameOracle	128→27.8	<b>28.1</b>	<b>33.8</b>	<b>77.3</b>	<b>69.0</b>	<b>65.2</b>	<b>69.1</b>	<b>72.3</b>	<b>66.3</b>	<b>60.1</b>
GPT-4o (Hurst et al., 2024)	16	-	-	<b>63.1</b>	-	51.6	58.5	66.0	<b>38.7</b>	55.6
+ FrameOracle	16→11.1	-	-	62.9	-	<b>52.1</b>	<b>59.2</b>	<b>68.8</b>	38.1	<b>56.2</b>

Under the 16-frame condition, FrameOracle maintains accuracy comparable to the baseline models across all benchmarks while reducing the number of frames by approximately 35%. With 64-frame inputs, FrameOracle begins with a denser candidate set and adaptively selects relevant frames. In this setting, it consistently improves performance over the baseline models while still reducing frames by about 15%. This demonstrates that a larger candidate pool enables FrameOracle to better exploit temporal redundancy, resulting in improved accuracy–efficiency trade-offs. FrameOracle is trained independently and applied in a fully plug-and-play manner, requiring no co-training or backbone-specific adaptation. These results confirm its ability to generalize across model architectures.

#### RQ 1: Does giving a VLM more frames consistently improve its performance?

One might expect that providing more frames always improves performance, since additional frames offer more visual evidence. However, Table 1 shows the opposite: using more frames often fails to help and can even reduce accuracy. This aligns with recent findings that long-video reasoning is inherently sparse, with only a small subset of frames being truly relevant (Park et al., 2024). Extra frames primarily introduce redundancy and noise, diluting cross-modal attention and yielding diminishing returns (Li et al., 2023).

By contrast, when FrameOracle selects a smaller but more informative subset of frames, performance can improve, especially on open-ended benchmarks. For example, on LLaVA-OneVision-7B, reducing 16 frames to roughly 10.4 improves NExTQA metrics (OE\_val: 14.6 → 16.1, OE\_test: 16.7 → 17.8) and EgoSchema (60.8 → 62.4). Similar trends are observed for GPT-4o, where accuracy rises from 55.6 to 56.2 despite using fewer frames. Qualitative examples in Appendix I (Figure 9) further illustrate this effect: FrameOracle identifies the key evidence with fewer frames, yielding correct answers where naive higher-frame sampling fails.

Crucially, this improvement does not come from simply reducing the visual input size. As shown in our ablation (Appendix F.3), uniformly sampling 10 frames from the same 16-frame input reduces performance substantially (49.8% → 46.3% on LLaVA-OneVision). In contrast, FrameOracle improves accuracy to 50.3% with the same 10-frame budget. This demonstrates that the gain comes from selecting semantically relevant frames, not from alleviating token overload.

#### RQ 2: How does FrameOracle compare with existing SOTA methods for keyframe selection?

We compare FrameOracle with (1) keyframe selection methods that are jointly trained with their VLM backbone in their original configurations, and (2) plug-and-play keyframe selection methods applied to open-source models (Table 2). The first category cannot be applied directly to open-source models, and FFS (Buch et al., 2025) is the only method that adaptively determines the number of

432 Table 2: **FrameOracle vs. SOTA keyframe selection methods.** NExTQA reports MCQ. Methods  
 433 using more frames or larger LLMs are shown in gray. LVB = LongVideoBench validation set.  
 434

435 Model	436 Frames	437 NExTQA	438 LVB	439 Video-MME	440 EgoSchema	441 MLVU
<i>(1) Jointly Trained Keyframe Selection Methods</i>						
437 SeViLA (Yu et al., 2023)	438 8	439 63.6	440 -	441 -	442 25.7	443 -
437 LVNet (Park et al., 2024)	438 12	439 72.9	440 -	441 -	442 -	443 -
437 VideoAgent (Wang et al., 2024)	438 8.4	439 71.3	440 -	441 -	442 60.2	443 -
437 FFS (Buch et al., 2025)	438 8.6	439 66.7	440 -	441 -	442 -	443 -
437 MoReVQA (Min et al., 2025)	438 30	439 69.2	440 -	441 -	442 -	443 -
437 VSLS (Guo et al., 2025)	438 32	439 -	440 63.4	441 63.0	442 -	443 -
437 AKS (Tang et al., 2025)	438 64	439 -	440 62.7	441 65.3	442 -	443 -
<i>(2) Plug-and-Play Keyframe Selection Methods</i>						
443 LLaVA-OneVision-7B (Li et al., 2025)	444 8	445 77.4	446 54.3	447 53.8	448 62.0	449 58.4
443 + Frame-Voyager (Yu et al., 2025)	444 128→8	445 73.9	446 -	447 <b>57.5</b>	448 -	449 <b>65.6</b>
443 + BOLT (Liu et al., 2025)	444 1fps→8	445 77.4	446 55.6	447 56.1	448 62.2	449 63.4
443 + KFC (Fang et al., 2025)	444 1fps→8	445 -	446 55.6	447 55.4	448 -	449 65.0
443 <b>+ FrameOracle</b>	444 64→8	445 <b>77.8</b>	446 <b>56.0</b>	447 <b>57.5</b>	448 <b>62.8</b>	449 62.9
443 LLaVA-Video-7B (Zhang et al., 2024)	444 8	445 75.6	446 54.2	447 55.9	448 51.8	449 60.5
443 + BOLT (Liu et al., 2025)	444 1fps→8	445 -	446 -	447 58.6	448 -	449 -
443 + KFC (Fang et al., 2025)	444 1fps→8	445 -	446 56.5	447 57.6	448 -	449 <b>66.9</b>
443 <b>+ FrameOracle</b>	444 64→8	445 <b>76.5</b>	446 <b>56.9</b>	447 <b>58.9</b>	448 <b>53.0</b>	449 63.4

451  
 452 Table 3: **Comparison of FLOPs, latency, visual tokens, and accuracy.** The values of the computational  
 453 cost are reported as per-GPU, per-sample averages.  
 454

455 Model	456 Frames	457 TFLOPs ↓				458 Latency (s) ↓	459 Visual Tokens ↓	460 Avg. Acc. ↑
		461 DINOv2	462 FrameOracle	463 VLM	464 Total			
457 LLaVA-Video-7B	458 16	459 -	460 -	461 184.38	462 184.38	463 0.615	464 11,644.0	465 54.6
457 + FrameOracle	458 16→10.4	459 1.87	460 $2.6 \times 10^{-4}$	461 <b>109.11</b>	462 <b>110.98</b>	463 <b>0.363</b>	464 <b>7,581.6</b>	465 54.7
457 + FrameOracle	458 64→13.9	459 7.58	460 $1.0 \times 10^{-3}$	461 160.09	462 167.67	463 0.556	464 10,133.1	465 <b>56.0</b>

461 retained frames; all other methods assume a fixed number of keyframes. All plug-and-play selection  
 462 methods only provided 8-frame results. To ensure a fair comparison, we disable FrameOracle’s K  
 463 Head and rely solely on the Rank Head: given 64 uniformly sampled frames, we select the top-8  
 464 ranked frames as input to the backbone VLMs.

465 FrameOracle achieves competitive performance compared to prior plug-and-play methods. Across  
 466 NExTQA, LongVideoBench, Video-MME, and EgoSchema, it improves accuracy by roughly 2–4  
 467 percentage points, outperforming Frame-Voyager (Yu et al., 2025), BOLT (Liu et al., 2025), and  
 468 KFC (Fang et al., 2025). On MLVU, FrameOracle outperforms the base VLMs but does not surpass  
 469 heuristic methods such as KFC, a greedy selection strategy that maximizes relevance and diversity,  
 470 which achieve higher scores. This gap reflects MLVU’s focus on fine-grained temporal grounding  
 471 and multi-event reasoning, where heuristics can sometimes capture domain-specific cues more ef-  
 472 fectively. Overall, the results demonstrate that even without the K Head, the Rank Head alone can  
 473 reliably prioritize important frames and deliver consistent gains across multiple VLMs, achieving  
 474 state-of-the-art performance on most benchmarks. **Beyond plug-and-play selectors, we also com-**  
 475 **pare FrameOracle with memory-based video compression methods such as MovieChat (Song et al.,**  
 476 **2024) on long-video benchmarks. As shown in Appendix F.6, when evaluated under the same down-**  
 477 **stream VLM (LLaVA-OneVision) and the same inference setup, FrameOracle achieves comparable**  
 478 **or better performance while using significantly fewer frames, highlighting its efficiency in handling**  
 479 **long temporal contexts.**

### 480 RQ 3: How much can FrameOracle reduce computational cost while preserving accuracy?

481 We take LLaVA-Video-7B with 16 input frames as the baseline and report per-GPU, per-sample  
 482 averages. FrameOracle reduces the input from 16 to 10.4 frames, cutting the VLM cost from 184.38  
 483 to 109.11 TFLOPs and the end-to-end total from 184.38 to 110.98 TFLOPs (−39.8%). It also  
 484 lowers latency from 0.615 to 0.363 seconds (−41.0%) and reduces tokens from 11,644.0 to 7,581.6,  
 485 while maintaining accuracy. With a larger candidate pool, FrameOracle reduces 64 frames to 13.9,  
 486 improving accuracy by +1.4 while still lowering total compute to 167.67 TFLOPs (−9.1%), tokens

486  
 487 **Table 4: Four-stage training of FrameOracle, evaluated on Qwen2.5-VL-3B.** Stages are added  
 488 progressively to assess their impact. The baseline (first row) randomly selects 16 of 32 frames. **Bold**  
 489 numbers indicate best performance. LVB = LongVideoBench validation set.

490 Model	491 Frames	492 NExTQA			493 Perception	494 LVB	495 Video-MME	496 EgoSchema	497 MLVU
		498 OE_val	499 OE_test	500 MC					
Qwen2.5-VL-3B	32→16	23.4	29.1	71.9	65.0	52.9	54.8	50.2	56.7
+ Stage 1	32→16	24.7	29.2	72.4	60.3	49.8	52.4	48.2	51.3
+ Stage 2	32→16	24.8	29.5	73.0	64.7	51.9	55.7	52.2	54.8
+ Stage 3	32→21.8	25.1	30.0	74.1	66.0	53.7	<b>59.4</b>	53.6	57.6
+ Stage 4	32→20.9	<b>25.6</b>	<b>30.5</b>	<b>74.8</b>	<b>66.7</b>	<b>54.3</b>	58.5	<b>53.8</b>	<b>58.4</b>

498 to 10,133.1 (−13.0%), and latency to 0.556 seconds (−9.6%). These results reveal a clear trade-  
 499 off: smaller frame pools yield larger efficiency gains without harming accuracy, while larger pools  
 500 provide accuracy improvements with moderate compute savings. Although this may appear to show  
 501 diminishing efficiency returns, roughly 90% of the total computation comes from the backbone  
 502 VLM. [As shown in Table 3, moving from the 16 → 10.4 to the 64 → 13.9 setting increases total](#)  
 503 [FLOPs almost entirely due to the VLM, while the selector accounts for only about 10%.](#) Similar  
 504 efficiency–accuracy trade-offs should hold for other ∼7B-scale models, with only minor variations  
 505 across architectures.

#### 506 **RQ 4: Are all training-stage components essential for FrameOracle’s performance?**

507 We conduct ablations over the four training stages to evaluate the contribution of each stage, using  
 508 Qwen2.5-VL-3B as the backbone VLM (Table 4). The baseline (first row) randomly selects 16  
 509 frames from 32 uniformly sampled candidates. Stage 1 (text–visual alignment) underperforms the  
 510 baseline, though it provides a foundational starting point. Stages 2 (Rank Head) and 3 (K Head) yield  
 511 clear performance improvements, and the full model with Stage 4 (fine-tuning on FrameOracle-41K)  
 512 delivers further gains over Stages 2 and 3 on most benchmarks, with only a slight decline on Video-  
 513 MME. Moreover, the average number of retained frames decreases from 21.8 to 20.9, showing that  
 514 FrameOracle-41K supervision stabilizes performance while enabling higher accuracy with fewer  
 515 frames. These results demonstrate that ground-truth supervision from FrameOracle-41K is essential  
 516 for refining both frame importance scoring and the prediction of the number of frames, establishing  
 517 it as a valuable resource for adaptive frame selection. [Furthermore, we validate the necessity of the](#)  
 518 [four-stage curriculum via two ablation studies. As detailed in Appendix F.1, we find that skipping](#)  
 519 [intermediate stages \(e.g., applying Stage 4 directly after Stage 1\) leads to overfitting and reduced](#)  
 520 [performance, while jointly optimizing Stage 2 and 3 results in training collapse and performance](#)  
 521 [drop due to mutual interference between the ranking and budgeting heads. These results confirm](#)  
 522 [that the progressive design is essential for both stable optimization and robust generalization.](#)

## 523 6 CONCLUSION

525 We propose FrameOracle, a lightweight, plug-and-play frame selector that adaptively determines  
 526 which frames to retain and how many are needed. To facilitate training, we introduce FrameOracle-  
 527 41K, a large-scale VideoQA dataset with 40,992 examples, and the first to provide keyframe an-  
 528 notations specifying the minimal frames required to answer each question. Experiments show that  
 529 FrameOracle improves diverse VLM backbones without co-training, reducing FLOPs, latency, and  
 530 token usage, while outperforming state-of-the-art keyframe selection methods. Future work will  
 531 explore supporting variable-sized frame inputs.

## 532 7 REPRODUCIBILITY STATEMENT

535 To support reproducibility, we provide details on both the model and dataset. FrameOracle’s design,  
 536 including its learning objective, selection policy, and staged curriculum, is described in Section 4,  
 537 with training procedures and hyperparameters in Appendix A (Figure 5; Table 5). FrameOracle-41K  
 538 construction, including agent-based mining, verification, and dataset format, is covered in Section 3  
 539 and Appendix B. Evaluation settings, including benchmarks, backbones, and metrics, are in Sec-  
 540 tion 5.1. These sections provide all the information needed to reproduce our results.

## 540 ETHICS STATEMENT

541

542 FrameOracle-41K is created from source videos collected from the internet, which may contain im-  
 543 ages of individuals and reflect societal biases present in online content. Our data processing pipeline  
 544 does not involve identifying or profiling any individuals. The data is used solely for developing our  
 545 video understanding model. We release the dataset strictly for non-commercial, academic research  
 546 purposes and caution future users to be aware of potential inherent biases in the data.

547

## 548 REFERENCES

549

550 Shuai Bai, Keqin Chen, Xuejing Liu, Jialin Wang, Wenbin Ge, Sibo Song, Kai Dang, Peng Wang,  
 551 Shijie Wang, Jun Tang, Humen Zhong, Yuanzhi Zhu, Mingkun Yang, Zhaohai Li, Jianqiang  
 552 Wan, Pengfei Wang, Wei Ding, Zheren Fu, Yiheng Xu, Jiabo Ye, Xi Zhang, Tianbao Xie, Zesen  
 553 Cheng, Hang Zhang, Zhibo Yang, Haiyang Xu, and Junyang Lin. Qwen2.5-vl technical report.  
 554 *arXiv:2502.13923*, 2025.

555

556 Shyamal Buch, Arsha Nagrani, Anurag Arnab, and Cordelia Schmid. Flexible frame selection for  
 557 efficient video reasoning. In *Proceedings of the IEEE/CVF Conference on Computer Vision and*  
 558 *Pattern Recognition (CVPR)*, 2025.

559

560 Chris Burges, Tal Shaked, Erin Renshaw, Ari Lazier, Matt Deeds, Nicole Hamilton, and Greg Hul-  
 561 lender. Learning to rank using gradient descent. In *Proceedings of the 22nd International Con-*  
 562 *ference on Machine Learning (ICML)*, 2005.

563

564 Keshigeyan Chandrasegaran, Agrim Gupta, Lea M. Hadzic, Taran Kota, Jimming He, Cristóbal  
 565 Eyzaguirre, Zane Durante, Manling Li, Jiajun Wu, and Li Fei-Fei. Hourvideo: 1-hour video-  
 566 language understanding. In *The Thirty-eighth Conference on Neural Information Processing Sys-*  
 567 *tems Datasets and Benchmarks Track (NeurIPS)*, 2024.

568

569 Jr-Jen Chen, Yu-Chien Liao, Hsi-Che Lin, Yu-Chu Yu, Yen-Chun Chen, and Yu-Chiang Frank Wang.  
 570 ReXTime: A benchmark suite for reasoning-across-time in videos. In *The Thirty-eighth Con-*  
 571 *ference on Neural Information Processing Systems Datasets and Benchmarks Track (NeurIPS)*,  
 572 2024a.

573

574 Lin Chen, Xilin Wei, Jinsong Li, Xiaoyi Dong, Pan Zhang, Yuhang Zang, Zehui Chen, Haodong  
 575 Duan, Bin Lin, Zhenyu Tang, Li Yuan, Yu Qiao, Dahua Lin, Feng Zhao, and Jiaqi Wang.  
 576 ShareGPT4video: Improving video understanding and generation with better captions. In *Pro-*  
 577 *ceedings of Thirty-eighth Conference on Neural Information Processing Systems Datasets and*  
 578 *Benchmarks Track (NeurIPS)*, 2024b.

579

580 Zesen Cheng, Sicong Leng, Hang Zhang, Yifei Xin, Xin Li, Guanzheng Chen, Yongxin Zhu, Wenqi  
 581 Zhang, Ziyang Luo, Deli Zhao, and Lidong Bing. Videollama 2: Advancing spatial-temporal  
 582 modeling and audio understanding in video-llms. *arXiv:2406.07476*, 2024.

583

584 Anxhelo Diko, Tinghuai Wang, Wassim Swaileh, Shiyan Sun, and Ioannis Patras. Rewind: Un-  
 585 derstanding long videos with instructed learnable memory. In *Proceedings of the IEEE/CVF*  
 586 *Conference on Computer Vision and Pattern Recognition (CVPR)*, 2025.

587

588 Sunqi Fan, Meng-Hao Guo, and Shuojin Yang. Agentic keyframe search for video question answer-  
 589 ing. *arXiv:2503.16032*, 2025.

590

591 Bo Fang, Wenhao Wu, Qiangqiang Wu, Yuxin Song, and Antoni B. Chan. Threading keyframe with  
 592 narratives: Mllms as strong long video comprehenders. *arXiv:2505.24158*, 2025.

593

594 Chaoyou Fu, Yuhang Dai, Yongdong Luo, Lei Li, Shuhuai Ren, Renrui Zhang, Zihan Wang, Chenyu  
 595 Zhou, Yunhang Shen, Mengdan Zhang, Peixian Chen, Yanwei Li, Shaohui Lin, Sirui Zhao, Ke Li,  
 596 Tong Xu, Xiawu Zheng, Enhong Chen, Caifeng Shan, Ran He, and Xing Sun. Video-mme:  
 597 The first-ever comprehensive evaluation benchmark of multi-modal llms in video analysis. In  
 598 *Proceedings of the IEEE/CVF Conference on Computer Vision and Pattern Recognition (CVPR)*,  
 599 2025.

600

601 Leo Gao, John Schulman, and Jacob Hilton. Scaling laws for reward model overoptimization. In  
 602 *Proceedings of the 40th International Conference on Machine Learning (ICML)*, 2022.

594 Weiyu Guo, Ziyang Chen, Shaoguang Wang, Jianxiang He, Yijie Xu, Jinhui Ye, Ying Sun, and Hui  
 595 Xiong. Logic-in-frames: Dynamic keyframe search via visual semantic-logical verification for  
 596 long video understanding. *arXiv:2503.13139*, 2025.

597

598 Kai Hu, Feng Gao, Xiaohan Nie, Peng Zhou, Son Tran, Tal Neiman, Lingyun Wang, Mubarak  
 599 Shah, Raffay Hamid, Bing Yin, and Trishul Chilimbi. M-llm based video frame selection for  
 600 efficient video understanding. In *Proceedings of the IEEE/CVF Conference on Computer Vision  
 and Pattern Recognition (CVPR)*, 2025.

601

602 Hang Hua, Yunlong Tang, Chenliang Xu, and Jiebo Luo. V2xum-llm: cross-modal video sum-  
 603 marization with temporal prompt instruction tuning. In *Proceedings of the Thirty-ninth AAAI  
 Conference on Artificial Intelligence (AAAI)*, 2025.

604

605 Aaron Hurst, Adam Lerer, Adam P. Goucher, Adam Perelman, Aditya Ramesh, Aidan Clark, AJ Os-  
 606 trow, Akila Welihinda, Alan Hayes, et al. Gpt-4o system card. *arXiv:2410.21276*, 2024.

607

608 Min Jung Lee, Dayoung Gong, and Minsu Cho. Video summarization with large language mod-  
 609 els. In *Proceedings of the IEEE/CVF Conference on Computer Vision and Pattern Recognition  
 (CVPR)*, 2025.

610

611 Jie Lei, Licheng Yu, Tamara Berg, and Mohit Bansal. TVQA+: Spatio-temporal grounding for  
 612 video question answering. In *Proceedings of the 58th Annual Meeting of the Association for  
 Computational Linguistics (ACL)*, 2020.

613

614 Bo Li, Yuanhan Zhang, Dong Guo, Renrui Zhang, Feng Li, Hao Zhang, Kaichen Zhang, Peiyuan  
 615 Zhang, Yanwei Li, Ziwei Liu, and Chunyuan Li. LLaVA-onevision: Easy visual task transfer.  
*Transactions on Machine Learning Research (TMLR)*, 2025.

616

617 Kunchang Li, Yali Wang, Yinan He, Yizhuo Li, Yi Wang, Yi Liu, Zun Wang, Jilan Xu, Guo Chen,  
 618 Ping Luo, Limin Wang, and Yu Qiao. Mvbench: A comprehensive multi-modal video under-  
 619 standing benchmark. In *Proceedings of the IEEE/CVF Conference on Computer Vision and Pattern  
 Recognition (CVPR)*, 2024a.

620

621 Yanwei Li, Chengyao Wang, and Jiaya Jia. Llama-vid: An image is worth 2 tokens in large language  
 622 models. In *Proceedings of the European Conference on Computer Vision (ECCV)*, 2024b.

623

624 Yi Li, Kyle Min, Subarna Tripathi, and Nuno Vasconcelos. Svitt: Temporal learning of sparse video-  
 625 text transformers. In *Proceedings of the IEEE/CVF Conference on Computer Vision and Pattern  
 Recognition (CVPR)*, 2023.

626

627 Hao Liang, Jiapeng Li, Tianyi Bai, Xijie Huang, Linzhuang Sun, Zhengren Wang, Conghui He,  
 628 Bin Cui, Chong Chen, and Wentao Zhang. Keyvideollm: Towards large-scale video keyframe  
 629 selection. *arXiv:2407.03104*, 2024.

630

631 Bin Lin, Yang Ye, Bin Zhu, Jiaxi Cui, Munan Ning, Peng Jin, and Li Yuan. Video-LLaVA: Learning  
 632 united visual representation by alignment before projection. In *Proceedings of the Conference on  
 633 Empirical Methods in Natural Language Processing (EMNLP)*, 2024a.

634

635 Ji Lin, Hongxu Yin, Wei Ping, Pavlo Molchanov, Mohammad Shoeybi, and Song Han. Vila: On pre-  
 636 training for visual language models. In *Proceedings of the IEEE/CVF Conference on Computer  
 637 Vision and Pattern Recognition (CVPR)*, June 2024b.

638

639 Tsung-Yi Lin, Michael Maire, Serge Belongie, Lubomir Bourdev, Ross Girshick, James Hays, Pietro  
 640 Perona, Deva Ramanan, C. Lawrence Zitnick, and Piotr Dollár. Microsoft coco: Common objects  
 641 in context. In *Proceedings of the European Conference on Computer Vision (ECCV)*, 2014.

642

643 Shuming Liu, Chen Zhao, Tianqi Xu, and Bernard Ghanem. Bolt: Boost large vision-language  
 644 model without training for long-form video understanding. In *Proceedings of the IEEE/CVF  
 Conference on Computer Vision and Pattern Recognition (CVPR)*, 2025.

645

646 Zhiqiang Lu, Zhenfei Yin, Mengwei He, Zhihui Wang, Zicheng Liu, Zhiyong Wang, and Kun Hu.  
 647 B-vllm: A vision large language model with balanced spatio-temporal tokens. In *Proceedings of  
 the IEEE/CVF International Conference on Computer Vision (ICCV)*, 2025.

648 Muhammad Maaz, Hanoona Rasheed, Salman Khan, and Fahad Khan. Video-ChatGPT: Towards  
 649 detailed video understanding via large vision and language models. In *Proceedings of the 62nd*  
 650 *Annual Meeting of the Association for Computational Linguistics (ACL)*, 2024.

651

652 Karttikeya Mangalam, Raiymbek Akshulakov, and Jitendra Malik. Egoschema: A diagnostic bench-  
 653 mark for very long-form video language understanding. In *Proceedings of Thirty-seventh Con-*  
 654 *ference on Neural Information Processing Systems Datasets and Benchmarks Track (NeurIPS)*,  
 655 2023.

656 Juhong Min, Shyamal Buch, Arsha Nagrani, Minsu Cho, and Cordelia Schmid. Morevqa: Explor-  
 657 ing modular reasoning models for video question answering. In *Proceedings of the IEEE/CVF*  
 658 *Conference on Computer Vision and Pattern Recognition (CVPR)*, 2025.

659 OpenGVLab. Internvl2: Better than the best—expanding performance boundaries of open-source  
 660 multimodal models with the progressive scaling strategy., 2024. URL <https://internvl.github.io/blog/2024-07-02-InternVL-2.0>.

661

662 Maxime Oquab, Timothée Darcet, Théo Moutakanni, Huy V. Vo, Marc Szafraniec, Vasil Khalidov,  
 663 Pierre Fernandez, Daniel HAZIZA, Francisco Massa, Alaaeldin El-Nouby, Mido Assran, Nicolas  
 664 Ballas, Wojciech Galuba, Russell Howes, Po-Yao Huang, Shang-Wen Li, Ishan Misra, Michael  
 665 Rabbat, Vasu Sharma, Gabriel Synnaeve, Hu Xu, Herve Jegou, Julien Mairal, Patrick Labatut,  
 666 Armand Joulin, and Piotr Bojanowski. DINov2: Learning robust visual features without super-  
 667 vision. *Transactions on Machine Learning Research (TMLR)*, 2024.

668

669 Jongwoo Park, Kanchana Ranasinghe, Kumara Kahatapitiya, Wonjeong Ryu, Donghyun Kim, and  
 670 Michael S. Ryoo. Too many frames, not all useful: Efficient strategies for long-form video qa.  
 671 *arXiv:2406.09396*, 2024.

672 Viorica Pătrăucean, Lucas Smaira, Ankush Gupta, Adrià Recasens Continente, Larisa Markeeva,  
 673 Dylan Banarse, Skanda Koppula, Joseph Heyward, Mateusz Malinowski, Yi Yang, Carl Doersch,  
 674 Tatiana Matejovicova, Yury Sulsky, Antoine Miech, Alex Frechette, Hanna Klimczak, Raphael  
 675 Koster, Junlin Zhang, Stephanie Winkler, Yusuf Aytar, Simon Osindero, Dima Damen, Andrew  
 676 Zisserman, and João Carreira. Perception test: A diagnostic benchmark for multimodal video  
 677 models. In *Proceedings of the Thirty-seventh Conference on Neural Information Processing Sys-*  
 678 *tems Datasets and Benchmarks Track (NeurIPS)*, 2023.

679 Rui Qian, Xiaoyi Dong, Pan Zhang, Yuhang Zang, Shuangrui Ding, Dahua Lin, and Jiaqi Wang.  
 680 Streaming long video understanding with large language models. In *Proceedings of the Thirty-*  
 681 *eighth Conference on Neural Information Processing Systems (NeurIPS)*, 2024.

682 QwenTeam. Qwen3-vl: Sharper vision, deeper thought, broader action, 2025. URL <https://qwen.ai/blog?id=99f0335c4ad9ff6153e517418d48535ab6d8afef>.

683

684 Ruchit Rawal, Khalid Saifullah, Miquel Farré, Ronen Basri, David Jacobs, Gowthami Somepalli,  
 685 and Tom Goldstein. Cinepile: A long video question answering dataset and benchmark.  
 686 *arXiv:2405.08813*, 2024.

687

688 Shuhuai Ren, Linli Yao, Shicheng Li, Xu Sun, and Lu Hou. Timechat: A time-sensitive multimodal  
 689 large language model for long video understanding. In *Proceedings of the IEEE/CVF Conference*  
 690 *on Computer Vision and Pattern Recognition (CVPR)*, 2024.

691 Enxin Song, Wenhao Chai, Guanhong Wang, Yucheng Zhang, Haoyang Zhou, Feiyang Wu, Haozhe  
 692 Chi, Xun Guo, Tian Ye, Yanting Zhang, Yan Lu, Jenq-Neng Hwang, and Gaoang Wang.  
 693 Moviechat: From dense token to sparse memory for long video understanding. In *Proceedings of*  
 694 *the IEEE/CVF Conference on Computer Vision and Pattern Recognition (CVPR)*, 2024.

695

696 Enxin Song, Wenhao Chai, Tian Ye, Jenq-Neng Hwang, Xi Li, and Gaoang Wang. Moviechat+:  
 697 Question-aware sparse memory for long video question answering. *IEEE Transactions on Pattern*  
 698 *Analysis and Machine Intelligence (TPAMI)*, 2025.

699 Nisan Stiennon, Long Ouyang, Jeff Wu, Daniel M. Ziegler, Ryan Lowe, Chelsea Voss, Alec Rad-  
 700 ford, Dario Amodei, and Paul Christiano. Learning to summarize from human feedback. In *Pro-*  
 701 *ceedings of the Thirty-fourth Conference on Neural Information Processing Systems (NeurIPS)*,  
 2020.

702 Kailong Tan, Yuxiang Zhou, Qianchen Xia, Rui Liu, and Yong Chen. Large model based sequential  
 703 keyframe extraction for video summarization. In *Proceedings of the International Conference on*  
 704 *Computing, Machine Learning and Data Science (CMLDS)*, 2024.

705

706 Xi Tang, Jihao Qiu, Lingxi Xie, Yunjie Tian, Jianbin Jiao, and Qixiang Ye. Adaptive keyframe sam-  
 707 pling for long video understanding. In *Proceedings of the IEEE/CVF Conference on Computer*  
 708 *Vision and Pattern Recognition (CVPR)*, 2025.

709 Xiaohan Wang, Yuhui Zhang, Orr Zohar, and Serena Yeung-Levy. Videoagent: Long-form video  
 710 understanding with large language model as agent. *arXiv:2403.10517*, 2024.

711

712 Haoning Wu, Dongxu Li, Bei Chen, and Junnan Li. Longvideobench: A benchmark for long-context  
 713 interleaved video-language understanding. In *Proceedings of the Thirty-eighth Conference on*  
 714 *Neural Information Processing Systems Datasets and Benchmarks Track (NeurIPS)*, 2024.

715

716 Junbin Xiao, Xindi Shang, Angela Yao, and Tat-Seng Chua. Next-qa:next phase of question-  
 717 answering to explaining temporal actions. In *Proceedings of the IEEE/CVF Conference on Com-*  
 718 *puter Vision and Pattern Recognition (CVPR)*, 2021.

719

720 Junbin Xiao, Nanxin Huang, Hangyu Qin, Dongyang Li, Yicong Li, Fengbin Zhu, Zhulin Tao,  
 721 Jianxing Yu, Liang Lin, Tat-Seng Chua, and Angela Yao. Videoqa in the era of llms: An empirical  
 722 study. *International Journal of Computer Vision (IJCV)*, 2025.

723

724 Tianwei Xiong, Yuqing Wang, Daquan Zhou, Zhijie Lin, Jiashi Feng, and Xihui Liu. LVD-2m: A  
 725 long-take video dataset with temporally dense captions. In *Proceedings of the Thirty-eighth Con-*  
 726 *ference on Neural Information Processing Systems Datasets and Benchmarks Track (NeurIPS)*,  
 727 2024.

728

729 An Yang, Baosong Yang, Binyuan Hui, Bo Zheng, Bowen Yu, Chang Zhou, Chengpeng Li,  
 730 Chengyuan Li, Dayiheng Liu, Fei Huang, Guanting Dong, Haoran Wei, Huan Lin, Jialong Tang,  
 731 Jialin Wang, Jian Yang, Jianhong Tu, Jianwei Zhang, Jianxin Ma, Jianxin Yang, Jin Xu, Jingren  
 732 Zhou, Jinze Bai, Jinzheng He, Junyang Lin, Kai Dang, Keming Lu, Keqin Chen, Kexin Yang,  
 733 Mei Li, Mingfeng Xue, Na Ni, Pei Zhang, Peng Wang, Ru Peng, Rui Men, Ruize Gao, Runji Lin,  
 734 Shijie Wang, Shuai Bai, Sinan Tan, Tianhang Zhu, Tianhao Li, Tianyu Liu, Wenbin Ge, Xiaodong  
 735 Deng, Xiaohuan Zhou, Xingzhang Ren, Xinyu Zhang, Xipin Wei, Xuancheng Ren, Xuejing Liu,  
 736 Yang Fan, Yang Yao, Yichang Zhang, Yu Wan, Yunfei Chu, Yuqiong Liu, Zeyu Cui, Zhenru  
 737 Zhang, Zhifang Guo, and Zhihao Fan. Qwen2 technical report. *arXiv:2407.10671*, 2024.

738

739 Zeyuan Yang, Delin Chen, Xueyang Yu, Maohao Shen, and Chuang Gan. Vca: Video curious agent  
 740 for long video understanding. *arXiv:2412.10471*, 2025.

741

742 Shoubin Yu, Jaemin Cho, Prateek Yadav, and Mohit Bansal. Self-chained image-language model  
 743 for video localization and question answering. In *Proceedings of the Thirty-seventh Conference*  
 744 *on Neural Information Processing Systems (NeurIPS)*, 2023.

745

746 Sicheng Yu, Chengkai Jin, Huanyu Wang, Zhenghao Chen, Sheng Jin, Zhongrong Zuo, Xiaolei Xu,  
 747 Zhenbang Sun, Bingni Zhang, Jiawei Wu, Hao Zhang, and Qianru Sun. Frame-voyager: Learning  
 748 to query frames for video large language models. In *Proceedings of the Thirteenth International*  
 749 *Conference on Learning Representations (ICLR)*, 2025.

750

751 Yuqian Yuan, Hang Zhang, Wentong Li, Zesen Cheng, Boqiang Zhang, Long Li, Xin Li, Deli Zhao,  
 752 Wenqiao Zhang, Yueting Zhuang, Jianke Zhu, and Lidong Bing. Videorefer suite: Advancing  
 753 spatial-temporal object understanding with video llm. In *Proceedings of the IEEE/CVF Confer-*  
 754 *ence on Computer Vision and Pattern Recognition (CVPR)*, 2025.

755

756 Xiaohua Zhai, Basil Mustafa, Alexander Kolesnikov, and Lucas Beyer. Sigmoid loss for language  
 757 image pre-training. In *Proceedings of the IEEE/CVF International Conference on Computer*  
 758 *Vision (ICCV)*, 2023.

759

760 Boqiang Zhang, Kehan Li, Zesen Cheng, Zhiqiang Hu, Yuqian Yuan, Guanzheng Chen, Sicong  
 761 Leng, Yuming Jiang, Hang Zhang, Xin Li, Peng Jin, Wenqi Zhang, Fan Wang, Lidong Bing, and  
 762 Deli Zhao. Videollama 3: Frontier multimodal foundation models for image and video under-  
 763 standing. *arXiv:2501.13106*, 2025a.

756 Hang Zhang, Xin Li, and Lidong Bing. Video-llama: An instruction-tuned audio-visual language  
 757 model for video understanding. In *Proceedings of the Conference on Empirical Methods in Nat-*  
 758 *ural Language Processing (EMNLP)*, 2023.

759

760 Kaichen Zhang, Bo Li, Peiyuan Zhang, Fanyi Pu, Joshua Adrian Cahyono, Kairui Hu, Shuai Liu,  
 761 Yuanhan Zhang, Jingkang Yang, Chunyuan Li, and Ziwei Liu. LMMs-eval: Reality check on the  
 762 evaluation of large multimodal models. In *Proceedings of the Conference of the Nations of the*  
*Americas Chapter of the Association for Computational Linguistics (NAACL)*, 2025b.

763

764 Ruohong Zhang, Liangke Gui, Zhiqing Sun, Yihao Feng, Keyang Xu, Yuanhan Zhang, Di Fu, Chun-  
 765 yuan Li, Alexander G Hauptmann, Yonatan Bisk, and Yiming Yang. Direct preference optimiza-  
 766 tion of video large multimodal models from language model reward. In *Proceedings of the Con-*  
*767 ference of the Nations of the Americas Chapter of the Association for Computational Linguistics*  
*(NAACL)*, 2025c.

768

769 Shaojie Zhang, Jiahui Yang, Jianqin Yin, Zhenbo Luo, and Jian Luan. Q-frame: Query-aware  
 770 frame selection and multi-resolution adaptation for video-llms. In *Proceedings of the IEEE/CVF*  
*771 International Conference on Computer Vision (ICCV)*, 2025d.

772

773 Yuanhan Zhang, Jinming Wu, Wei Li, Bo Li, Zejun Ma, Ziwei Liu, and Chunyuan Li. Video  
 774 instruction tuning with synthetic data. *arXiv:2410.02713*, 2024.

775

776 Long Zhao, Nitesh B. Gundavarapu, Liangzhe Yuan, Hao Zhou, Shen Yan, Jennifer J. Sun, Luke  
 777 Friedman, Rui Qian, Tobias Weyand, Yue Zhao, Rachel Hornung, Florian Schroff, Ming-Hsuan  
 778 Yang, David A. Ross, Huisheng Wang, Hartwig Adam, Mikhail Sirotenko, Ting Liu, and Boqing  
 779 Gong. Videoprism: A foundational visual encoder for video understanding. In *Proceedings of the*  
*42nd International Conference on Machine Learning (ICML)*, 2024.

780

781 Junjie Zhou, Yan Shu, Bo Zhao, Boya Wu, Zhengyang Liang, Shitao Xiao, Minghao Qin, Xi Yang,  
 782 Yongping Xiong, Bo Zhang, Tiejun Huang, and Zheng Liu. Mlvu: Benchmarking multi-task  
 783 long video understanding. In *Proceedings of the IEEE/CVF Conference on Computer Vision and*  
*784 Pattern Recognition (CVPR)*, 2025.

785

786

787

788

789

790

791

792

793

794

795

796

797

798

799

800

801

802

803

804

805

806

807

808

809

## APPENDIX

## A FULL IMPLEMENTATION DETAILS

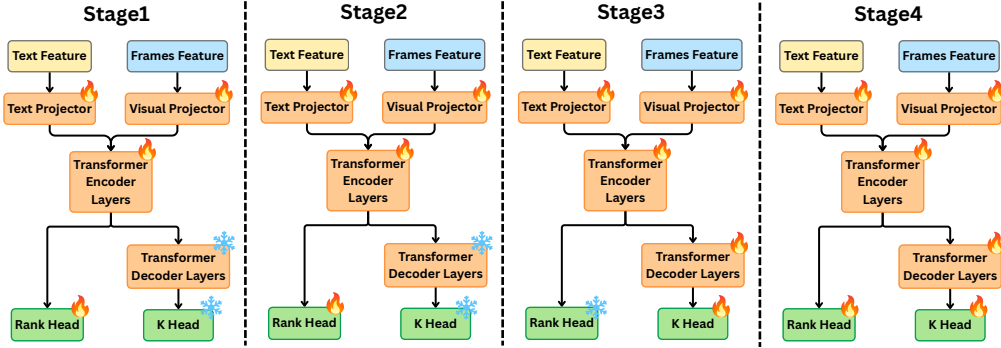


Figure 5: **Four-stage training strategy of FrameOracle.** The model is progressively optimized from weak to strong supervision, culminating in supervised fine-tuning with FrameOracle-41K annotations. Fire icons indicate trainable modules, while snowflake icons denote frozen ones.

Table 5: **Datasets used in FrameOracle training.** Stage 4 leverages FrameOracle-41K.

Task	Dataset	Amount
Stage1	LLaVA-Video-178K (Zhang et al., 2024), ShareGPT4o-Video (Chen et al., 2024b), Video-ChatGPT (Maaz et al., 2024)	300K
Stage2	LLaVA-Video-178K (Zhang et al., 2024), LLaVA-Hound (Zhang et al., 2025c), Video-ChatGPT (Maaz et al., 2024)	300K
Stage3	LLaVA-Video-178K (Zhang et al., 2024), LLaVA-Hound (Zhang et al., 2025c), Video-ChatGPT (Maaz et al., 2024)	300K
Stage4	<b>FrameOracle-41K (Our Dataset)</b>	40K

**Training strategy illustration.** Figure 5 presents a schematic of our four-stage curriculum, highlighting trainable modules (fire) and frozen modules (snowflake) at each stage.

**Hardware and input budgets.** All training is conducted on  $8 \times \text{H100}$  GPUs. We train two FrameOracle variants: one with 16 uniformly sampled candidate frames and another with 64. A cosine learning rate scheduler with the AdamW optimizer is used across all stages.

**Datasets used in staged training.** FrameOracle is optimized using a four-stage curriculum with progressively stronger supervision. Stages 1-3 rely on large-scale video-language corpora, while Stage 4 leverages our FrameOracle-41K dataset. Table 5 summarizes the dataset composition for each stage.

**Stage 1: Cross-modal alignment.** K Head is frozen while the feature projectors and cross-modal Transformer encoder are trained jointly, both optimized with a learning rate of  $1 \times 10^{-4}$ . The 16-frame selector uses a batch size of 16 and trains for approximately 48 hours, whereas the 64-frame version uses a smaller batch size of 2 and completes in about 91 hours.

**Stage 2: Rank Head optimization.** Rank Head is trained while the K Head remains frozen. The Rank Head uses a learning rate of  $1 \times 10^{-4}$ , and the feature projectors and Transformer encoder are fine-tuned with a smaller learning rate of  $1 \times 10^{-5}$ . The 16-frame selector uses a batch size of 16 and trains for approximately 40 hours, whereas the 64-frame variant uses the same batch size and takes about 52 hours.

**Stage 3: K Head optimization.** K Head is the primary trainable module, optimized with a learning rate of  $1 \times 10^{-4}$ . The feature projectors and Transformer encoder are lightly updated with a learning rate of  $1 \times 10^{-7}$ , while the Rank Head remains frozen. We set  $\lambda_k = 0.0105$  to balance accuracy

864 and efficiency. The 16-frame selector uses a batch size of 16 and trains for approximately 35 hours,  
 865 whereas the 64-frame variant uses the same batch size and takes about 60 hours.  
 866

867 **Stage 4: Supervised fine-tuning on FrameOracle-41K.** Rank Head and K Head are trained jointly  
 868 with a learning rate of  $5 \times 10^{-5}$ , while the feature projectors and Transformer encoder are fine-tuned  
 869 with  $1 \times 10^{-5}$ . The 16-frame selector is trained with a batch size of 8 for approximately 12 hours,  
 870 and the 64-frame version uses the same batch size and trains for about 18 hours.  
 871

## 872 B FRAMEORACLE-41K DATA FORMAT

874 We release the FrameOracle-41K dataset in JSON format, with each entry corresponding to a single  
 875 video-question pair. Each entry includes the instance identifier, question-answer pair, paths to the  
 876 associated video and extracted keyframes, video duration, and number of selected frames. Below,  
 877 we provide an example JSON entry to illustrate the dataset’s structure.

```
878 {
879   "id": 30,
880   "question": "What folding technique is demonstrated first in the video?
881   ",
882   "ground_truth_answer": "The 'SHIKAKU NO GI' (Square Fold) technique is
883   demonstrated first.",
884   "video": "/srv/nfs/video_data/video/ytb_8yhoV5C3bT8.mp4",
885   "keyframes_dir": "/srv/nfs/video_data/extracted_frames/ytb_8yhoV5C3bT8"
886   ,
887   "duration": 126.893,
888   "num_selected_frames": 8
}
```

## 890 C PROMPTS FOR DATA GENERATION

### 893 Prompt Template for Stage I: Initial Frame Analysis

895 You are analyzing a video that is {duration\_seconds} seconds long. The video has been  
 896 uniformly sampled into 64 frames, indexed from 0 (start) to 63 (end).

897 Analyze these {len(initial\_indices)} initial frames (indices: {initial\_indices}) to answer:  
 898 “{question}”. Provide a short caption for each frame, a relevance score (INTEGER 1-5),  
 899 your confidence (high/medium/low), and your answer attempt.  
 900

901 Respond in JSON: {{“frame\_analysis”: [{“index”: int, “caption”: “str”, “relevance”: int}], “confidence”: “str”, “answer\_attempt”: “str”, “reasoning”: “str”}}

### 903 IMPORTANT GUIDELINES:

- 905 - Relevance combines BOTH
  - 906 (a) how well the frame’s TEMPORAL POSITION matches the question mentioned, and
  - 907 (b) how much the visible CONTENT answers the question. A high score (4-5) requires
  - 908 strong evidence on both axes.
- 909 - You may use “high” confidence early ONLY IF: You have seen explicit, definitive evidence
- 910 that unquestionably answers the question (e.g., clearly visible target object/person/action).
- 911 - Before setting “high” confidence, explicitly mention in your reasoning:
  - 912 (a) Why current evidence is sufficient.
  - 913 (b) Why additional unseen frames are unlikely to alter your conclusion.
- 914 - If there’s any reasonable scenario where unseen frames could alter your answer, you must
- 915 explicitly acknowledge that and keep your confidence at “medium”.

916 **Follow these instructions strictly.**

918  
919**Prompt Template for Stage II: Deep-dive Analysis and Refinement**920  
921  
922

You are analyzing a video that is  $\{\text{duration\_seconds}\}$  seconds long. The video has been uniformly sampled into 64 frames, indexed from 0 (start) to 63 (end).

923  
924  
925

Current context on question “ $\{\text{question}\}$ ”:

Current context in buffer “ $\{\text{buffer}\}$ ”.

926  
927

Now analyze these  $\{\text{len}(\text{indices})\}$  new frames (indices:  $\{[\text{int}(\text{idx}) \text{ for } \text{idx} \in \text{indices}]\}$ ) from the gap ( $\{\text{start\_idx}\}$ ,  $\{\text{end\_idx}\}$ ).

928

**Tasks:**929  
930

- Provide a caption, relevance score (INTEGER 1-5) for each NEW frame, your UPDATED confidence, answer, and reasoning.
- If the new evidence changes your view of any PREVIOUS frame listed above, list the updated scores under “ $\{\text{revised\_prev\_scores}\}$ ” (index, new relevance 1-5).

933  
934  
935  
936  
937

Respond in JSON:  $\{ \{ \{ \text{“new\_frame\_analysis”} : [ \{ \{ \{ \text{“index”} : \text{int}, \text{“caption”} : \text{“str”}, \text{“relevance”} : \text{int} \} \}, \text{“revised\_prev\_scores”} : [ \{ \{ \{ \text{“index”} : \text{int}, \text{“relevance”} : \text{int} \} \}, \text{“confidence”} : \text{“str”}, \text{“answer\_attempt”} : \text{“str”}, \text{“reasoning”} : \text{“str”} \} \} ] \} \} \}$

938  
939**D ADDITIONAL DATASET STATISTICS**940  
941  
942  
943  
944

To complement the main dataset description, we provide additional statistics that illustrate the textual and visual properties of FrameOracle-41K. Table 6 lists the 16 question types and their associated definitions, while Figure 6 visualizes several key quantitative aspects of the dataset.

945  
946

Table 6: Question types and their corresponding definitions in FrameOracle-41K.

Question type	Definition
Temporal	Designed to assess reasoning about temporal relationships between actions or events. Questions involve previous, present, or next actions.
Spatial	Tests ability to perceive spatial relationships between observed instances in a video scene.
Causal	Focuses on explaining actions or events and determining intentions, causes, or consequences.
Description Scene	Assesses ability to describe the major scene of the video, such as where it takes place and the overall environment.
Description Human	Involves describing actions or attributes of people, such as their activities and appearances.
Description Object	Assesses ability to describe attributes of objects, including appearance and function.
Count	Tests ability to count instances of objects, people, or actions, and to distinguish between old and new elements in a scene.
Binary	Involves yes/no questions related to the video content.
Fine-Grained Action	Creates questions that challenge comprehension of subtle or detailed actions.
Plot	Challenges ability to interpret the narrative or plot in the video.
Object Existence	Assesses reasoning with introduced non-existent activities while keeping physical scene details unchanged.
Time Order	Challenges recognition of the temporal sequence of activities in videos.
Object Direction	Emphasizes perception of object movement direction.
Camera Direction	Focuses on the direction of camera movement.
Speed	Delves into discerning variations in motion speed, including absolute and relative differences.
Attribute Change	Centers on how object or scene attributes change over time, such as size, shape, color, or other properties.

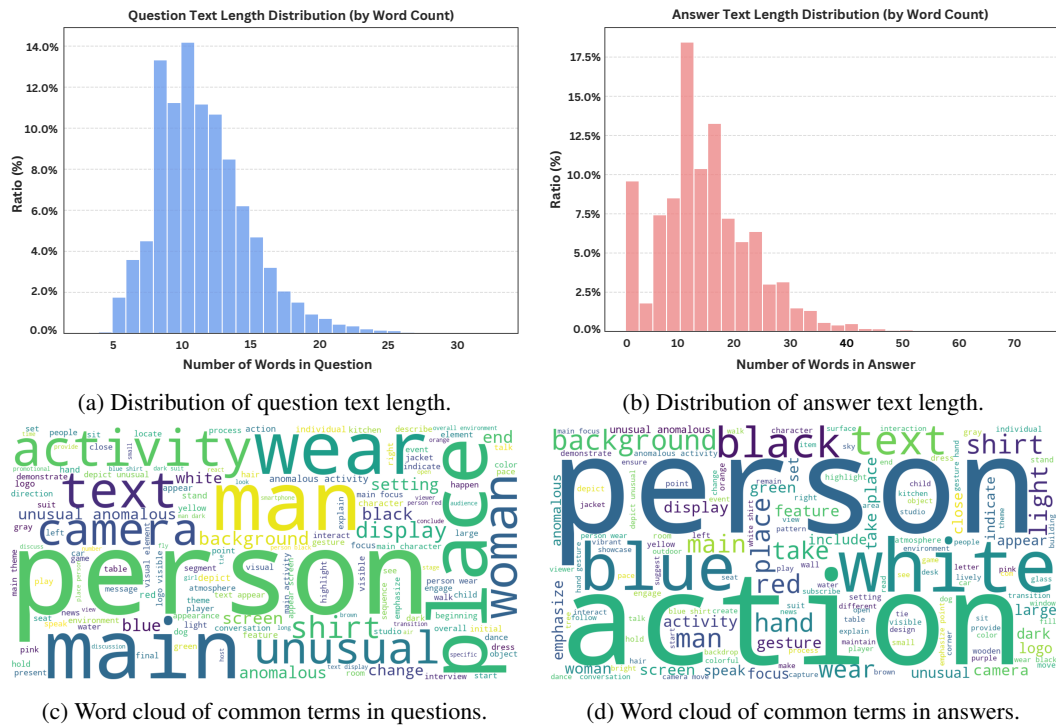


Figure 6: **Additional dataset statistics.** (a) Distribution of question lengths. Most questions are short, typically ranging from 6 to 15 words. (b) Distribution of answer lengths. Answers show a slightly higher variance, indicating that some responses are longer or more descriptive. (c) Word cloud constructed from all questions, highlighting frequently used terms related to subjects, scenes, and activities. (d) Word cloud constructed from all answers, highlighting frequently used terms related to appearance, objects, and actions.

Figure 6a shows that most questions are short, typically between six and fifteen words, peaking around ten. This reflects our design goal of keeping each question focused on a single aspect of the video. Figure 6b shows answer lengths, which are generally similar to the questions but slightly more variable: most are short, yet some extend into longer, descriptive phrases. Together, these figures indicate that questions and answers are mostly compact, while answers allow some variation, supporting models in producing both concise labels and richer, sentence-level responses.

Figure 6c shows a word cloud of all questions. Frequent terms like person, place, activity, and wear indicate that questions often focus on subjects, scenes, and actions, reflecting diverse reasoning types in the dataset. Figure 6d shows a word cloud of all answers, where common words such as person, action, and various color terms highlight the focus on actions, appearances, objects, and scene details.

Together, these statistics provide a clear picture of FrameOracle’s composition and design. Questions and answers remain concise yet varied, capturing both factual and descriptive reasoning. Videos provide sufficient temporal coverage without redundancy, and the lexical patterns demonstrate a balanced emphasis on visual grounding and action understanding.

## E HUMAN VERIFICATION OF FRAMEORACLE-41K ANNOTATIONS

To ensure the reliability of FrameOracle-41K’s automatically generated annotations, we conduct a human verification study on 4,000 randomly sampled instances ( $\approx 10\%$  of the dataset). Ten independent annotators participate, with each sample reviewed by two distinct annotators. A sample is considered correct only if both annotators can answer the question using only the provided keyframes, without access to the full video or ground-truth answer. Inter-annotator agreement is high, at 94%, indicating strong consistency. As shown in Table 7, the overall human-verified accuracy is 93.3%.

1026 Table 7: Distribution of pairwise annotation outcomes on the human verification set (4,000 samples).  
 1027 A sample is classified as “Both correct” if both annotators answered the question correctly using the  
 1028 provided keyframes, “One correct / one wrong” if exactly one annotator answered correctly, and  
 1029 “Both wrong” if neither annotator answered correctly.

Annotator Agreement Category	Count	Percentage
Both correct	3,732	93.3%
One correct / one wrong	240	6.0%
Both wrong	28	0.7%

1035  
 1036 Table 8: **Human verification on frame sufficiency.** We classify the annotated keyframe sets into  
 1037 three categories based on the gap between the annotated count and the human-perceived minimal  
 1038 sufficiency.

Category	Criterion	Count	Percentage
Excessive	$\geq 5$ frames beyond minimal sufficiency	3,628	97.2%
Just-right	within $\pm 4$ frames of minimal sufficiency	98	2.6%
Insufficient	Missing critical evidence	6	0.2%

1045  
 1046 (3,732/4,000), confirming that the vast majority of mined keyframe sets provide sufficient evidence  
 1047 for human-level reasoning.

1048 Beyond correctness, we assess whether the annotated frames follow the principle of “minimal sufficiency.” For all verified samples, annotators label keyframe sets as *Excessive*, *Just-right*, or *Insufficient*. Table 8 provides detailed definitions and statistics. As shown, the vast majority of samples (97.2%) are *Just-right*, with only a small fraction classified as excessive or insufficient. This confirms that FrameOracle-41K provides high-quality supervision that is both semantically accurate and frame-efficient, validating the effectiveness of our automated multi-stage generation pipeline.

## F ADDITIONAL ABLATION STUDIES AND ANALYSIS

1055  
 1056 In this section, we present ablation studies and comparative analyses to validate FrameOracle’s ar-  
 1057 chitectural and methodological choices. We examine six key aspects to highlight the robustness and  
 1058 efficiency of our approach: (1) the **necessity of the multi-stage training curriculum**, showing that  
 1059 intermediate weak supervision is crucial for avoiding overfitting and learning generalized policies;  
 1060 (2) the **impact of the supervision backbone**, demonstrating that the selector generalizes across  
 1061 different teacher models and effectively leverages stronger visual representations to enhance long-  
 1062 context reasoning; (3) the **source of performance gains**, confirming through equal-budget com-  
 1063 parisons that improvements come from selecting semantically relevant frames rather than simply  
 1064 reducing visual input; (4) the **stability of freezing the Rank Head**, verifying that ranking consis-  
 1065 tency is preserved in Stage 3 and fully refined by subsequent fine-tuning in Stage 4; (5) the benefits  
 1066 of **frame-level over token-level budgeting**, demonstrating that maintaining whole-frame integrity  
 1067 outperforms rigid token limits; and (6) the advantage of **explicit selection over memory compres-**  
 1068 **sion**, with substantial gains over long-video compression baselines. Together, these results show that  
 1069 FrameOracle’s effectiveness stems from intelligent, query-conditioned semantic frame selection.

### F.1 NECESSITY OF THE MULTI-STAGE TRAINING CURRICULUM

1071  
 1072 Our training pipeline adopts a specific four-stage curriculum. To validate this design, we conduct  
 1073 two complementary ablation studies using the Qwen2.5-VL-3B backbone: (1) investigating whether  
 1074 intermediate weak supervision stages can be skipped (Stage 1+4), and (2) examining whether they  
 1075 can be merged into a single joint optimization step (Joint Training).

1076  
 1077 **Can we skip the intermediate stages?** To assess whether the four-stage curriculum is necessary or  
 1078 if the model could learn solely from Stage 4’s strong supervision (FrameOracle-41K), we perform an  
 1079 ablation that compare the full pipeline against a simplified version using only Stage 1 (Text–Visual

1080 Table 9: **Ablation of training stages.** Results are reported on Qwen2.5-VL-3B with 32 candidate  
 1081 frames. Average accuracy is calculated across all benchmarks listed in Table 1.

1083 <b>Setting</b>	1084 <b>Frame Selection</b>	1085 <b>Avgverage Accuracy</b>
1084 Qwen2.5-VL-3B (Baseline)	1085 32	1086 50.5
1085 + Stage 1	1086 32 → 16	1087 48.5
1086 + Stage 1+4 (Fixed K)	1087 32 → 16	1088 49.6
1087 + Stage 1+2	1088 32 → 16	1089 50.8
1088 + Stage 1+4 (Adaptive K)	1089 32 → 13.4	1090 46.9
1089 + <b>Full (Stage 1–4)</b>	1090 <b>32 → 20.9</b>	1091 <b>52.8</b>

1091 Table 10: **Joint Training vs. Staged Training.** Comparison of downstream performance with a  
 1092 fixed 16-frame budget.

1094 <b>Training Strategy</b>	1095 <b>Frames</b>	1096 <b>NEXTQA</b>			1097 <b>Perception</b>	1098 <b>LVB</b>	1099 <b>Video-MME</b>	1100 <b>EgoSchema</b>	1101 <b>MLVU</b>
		1102 <b>OE_val</b>	1103 <b>OE_test</b>	1104 <b>MC</b>					
1106 Stage 2+3 (joint)	1107 32→16	1108 24.0	1109 27.8	1110 72.2	1111 63.8	1112 50.1	1113 54.3	1114 49.8	1115 52.2
1116 Stage 2 alone	1117 32→16	1118 <b>24.8</b>	1119 <b>29.5</b>	1120 <b>73.0</b>	1121 <b>64.7</b>	1122 <b>51.9</b>	1123 <b>55.7</b>	1124 <b>52.2</b>	1125 <b>54.8</b>

1100 Alignment) and Stage 4 (Supervised Fine-tuning), evaluating two settings: (1) fixed  $K$  and (2) adaptive  $K$  prediction. As Table 9 shows, skipping intermediate stages reduces performance. Stage 1+4  
 1101 improves over Stage 1 alone but still falls short of the Stage 1+2 baseline. Notably, enabling the K  
 1102 Head without Stage 3 calibration (Adaptive K) drops average accuracy to 46.9% and causes over-  
 1103 fitting to FrameOracle-41K’s statistics. These results confirm that the weak supervision in Stages 2  
 1104 and 3 is crucial for learning generalized ranking and frame-budget policies before refinement with  
 1105 ground-truth annotations.

1107 **Can we jointly train Stage 2 and 3?** We further investigate whether Stage 2 (Rank optimization)  
 1108 and Stage 3 (K optimization) could be simplified into a single joint training phase. We train a variant  
 1109 where both heads are optimized simultaneously. We observe severe optimization instability under  
 1110 the joint setting. Specifically, the K Head collapses, predicting near-maximum frames (i.e., failing  
 1111 to perform meaningful frame reduction), and the Rank Head becomes unstable, with Kendall- $\tau$   
 1112 fluctuating between -0.4 and +0.6. This instability arises because the two objectives interfere during  
 1113 joint optimization: immature Rank predictions generate noisy top-K subsets that destabilize K-Head  
 1114 learning, and the resulting unstable K outputs further corrupt Rank learning, creating a feedback  
 1115 loop that prevents either head from converging. To quantify the impact, we measure the ranking  
 1116 consistency (Kendall- $\tau$ ) against ground truth and evaluate downstream performance under a fixed  
 1117 16-frame budget (to isolate ranking quality).

1118 As shown in Table 10, the jointly trained model achieves a Kendall- $\tau$  of only **0.2313** (vs. 0.5367  
 1119 for Stage 2 alone) and consistently underperforms the staged baseline across all benchmarks. These  
 1120 results confirm that decoupling the ranking and budgeting objectives via a curriculum is essential  
 1121 for stable optimization.

## 1122 F.2 IMPACT OF THE SUPERVISION BACKBONE

1124 In our default setting, Stages 2 and 3 use Qwen2.5-VL-3B (Bai et al., 2025) to provide soft supervi-  
 1125 sion (via VLM loss) for training the Rank Head and K Head. To assess whether FrameOracle relies  
 1126 on specific architectural biases of the teacher model, we conduct an ablation by replacing Qwen2.5-  
 1127 VL-3B with the more powerful VideoLLaMA3-7B (Zhang et al., 2025a) during training. To ensure  
 1128 a controlled comparison, both selector variants are evaluated using the same downstream pipeline  
 1129 (LLaVA-OneVision-7B (Li et al., 2025)) on the same benchmarks.

1130 As shown in Table 11, replacing the backbone has minimal effect on the predicted frame counts,  
 1131 with both selectors producing nearly identical values (13.9 versus 14.2). Crucially, both variants  
 1132 outperform the full-frame baseline, demonstrating that FrameOracle generalizes well across differ-  
 1133 ent visual backbones. Furthermore, the selector trained with VideoLLaMA3-7B achieves stronger  
 1134 performance across benchmarks. This improvement stems from VideoLLaMA3-7B’s stronger vi-

1134 Table 11: Comparison of FrameOracle models trained with different VLM backbones (Stage 2/3).  
1135

Model	Frames	NExTQA			Perception	LVB	Video-MME	EgoSchema	MLVU
		OE_val	OE_test	MC					
LLaVA-OneVision-7B	16	14.6	16.7	78.2	56.4	55.0	56.1	60.8	60.9
+ FrameOracle (VideoLLaMA3-7B)	13.9	16.5	<b>19.0</b>	<b>78.5</b>	56.9	56.5	58.1	63.4	63.7
+ FrameOracle (Qwen2.5-VL-3B)	14.2	<b>16.7</b>	18.9	<b>78.5</b>	<b>57.0</b>	<b>57.4</b>	<b>58.4</b>	<b>64.0</b>	<b>65.1</b>

1140

1141

1142 Table 12: Evaluation on LLaVA-OneVision-7B under an equal frame budget.  
1143

Model	Frames	NExTQA			Perception	LVB	Video-MME	EgoSchema	MLVU	Avg.
		OE_val	OE_test	MC						
LLaVA-OneVision-7B	16 → 10 (Uniform)	8.8	11.5	73.5	53.8	53.2	54.1	60.0	55.8	46.3
+ FrameOracle	<b>16 → 10.4</b>	<b>16.1</b>	<b>17.8</b>	<b>77.6</b>	<b>56.5</b>	<b>55.5</b>	<b>56.0</b>	<b>62.4</b>	<b>60.2</b>	<b>50.3</b>

1147

1148

1149 sual representations, which provide richer information about events spanning longer periods; as a  
1150 result, this selector is better at choosing frames that capture high-level or long-range context, leading  
1151 to larger gains on long-video benchmarks (e.g., MLVU).  
1152

1153

1154 F.3 DO FRAMEORACLE’S GAINS COME FROM FEWER FRAMES OR BETTER FRAMES?  
11551156 We assess whether FrameOracle’s improvement over the full-frame baseline comes from better  
1157 frame selection rather than simply using fewer frames. To do this, we compare FrameOracle with  
1158 a uniform sampling baseline under the same frame budget. Using LLaVA-OneVision-7B, Frame-  
1159 Oracle reduces 16 input frames to an average of 10.4. We then uniformly sample 10 frames from  
1160 the same 16-frame inputs and evaluate both on the same benchmarks. As Table 12 shows, uni-  
1161 form sampling achieves 46.3% average accuracy, while FrameOracle reaches 50.3%. This 4.0-point  
1162 gain confirms that the improvement comes from selecting semantically relevant, query-conditioned  
1163 frames, not merely from reducing the number of frames.  
1164

1165

1166 F.4 EFFECT OF FREEZING THE RANK HEAD IN STAGE 3  
11671168 We evaluate how freezing the Rank Head during Stage 3, while updating the Transformer encoder  
1169 layers, affects its alignment with the evolving frame representations. This alignment is crucial for  
1170 accurately ranking frames, especially in long videos where subtle differences in importance matter.  
1171 To assess this, we perform a dedicated ablation measuring both (1) ranking consistency and (2)  
1172 downstream task performance.  
1173

1174

1175 **Frame-Importance Consistency.** We randomly sample 500 training videos and compute a  
1176 “ground-truth” importance distribution using leave-one-out (LOO) VLM loss. We then evaluate  
1177 how well the Rank Head from Stages 2, 3, and 4 aligns with this distribution using Kendall- $\tau$  corre-  
1178 lation. A large drop from Stage 2 to Stage 3 would indicate that freezing the Rank Head reduces its  
1179 ability to track the encoder’s evolving representations. As Table 13 shows,  $\tau$  decreases only slightly  
1180 after Stage 3. This is largely due to the very low learning rate ( $1 \times 10^{-7}$ ) used for encoder updates,  
1181 which limits feature drift. Stage 4 fully restores and even improves the alignment, demonstrating  
1182 that any temporary misalignment is easily corrected through supervised fine-tuning.  
1183

1184

1185

1186

1187

1188 **Downstream Benchmark Evaluation.** We assess the practical impact of freezing the Rank Head in  
1189 Stage 3 by evaluating Stages 2, 3, and 4 on video benchmarks using the Qwen2.5-VL-3B backbone  
1190 with 32-frame inputs. To ensure a controlled comparison, we fix the number of selected frames to  
1191 16 across all stages, isolating the effect of ranking drift. As shown in Table 14, Stage 3 performs on  
1192 par with Stage 2, indicating that the temporary freeze causes only negligible drift. Stage 4 consistently  
1193 boosts performance across all benchmarks, confirming that supervised fine-tuning effectively  
1194 realigns and strengthens the ranking behavior. These results demonstrate that temporarily freezing  
1195 the Rank Head does not meaningfully harm the selector, even in long-video scenarios where ranking  
1196 stability is critical.  
1197

1188 Table 13: Kendall- $\tau$  consistency across training stages.  
1189

Model	Kendall- $\tau$ (vs. Ground Truth)
Stage 2	0.5367
Stage 3	0.5221
Stage 4	<b>0.5833</b>

1196 Table 14: Downstream performance across training stages under a fixed 16-frame selection.  
1197

Model	Frames	NExTQA			Perception	LVB	Video-MME	EgoSchema	MLVU	Avg.
		OE_val	OE_test	MC						
Stage 2	32→16	24.8	29.5	73.0	64.7	51.9	55.7	52.2	54.8	50.8
Stage 3	32→16	24.8	29.5	72.7	64.9	52.0	56.0	51.8	54.4	50.8
Stage 4	32→16	<b>25.3</b>	<b>30.0</b>	<b>74.0</b>	<b>65.8</b>	<b>52.9</b>	<b>56.9</b>	<b>52.8</b>	<b>55.5</b>	<b>51.7</b>

## 1204 F.5 FRAME-LEVEL VS. TOKEN-LEVEL INFORMATION BUDGETING

1206 An important question in adaptive video understanding is how to define the unit of computational  
1207 budget: by visual tokens or by frames. To investigate this, we compare two representative strategies:  
1208

- **Token-level Budgeting:** Operates at a fine-grained level, selecting specific spatial-temporal tokens to fit a **fixed** total budget. This may discard parts of a frame to save computation.
- **Frame-level Budgeting (Ours):** Operates at a coarser granularity, treating each frame as an atomic unit. It **dynamically predicts** a budget of  $K$  full frames, preserving the complete spatial context of each selected frame.

1209 To compare these strategies, we select B-VLLM (Lu et al., 2025) as a representative token-level  
1210 budgeting method. B-VLLM samples videos at 1 fps and enforces a fixed budget of 512 visual  
1211 tokens, selecting the most relevant spatial tokens across the sequence. We compare this against  
1212 FrameOracle, which predicts a dynamic number of frames. For a fair comparison, we evaluate both  
1213 methods under a unified backbone (VideoLLaMA2 (Cheng et al., 2024)) to isolate the effect of the  
1214 selection mechanism. Additionally, we compare B-VLLM’s best-reported performance with our  
1215 LLaVA-Video integration, both using Qwen2 (Yang et al., 2024) as the backbone LLM. As shown  
1216 in Table 15, FrameOracle consistently outperforms B-VLLM across all benchmarks. These results  
1217 indicate that preserving the spatial integrity of frames is crucial for reasoning and that dynamically  
1218 selecting the number of frames is a more effective approach for controlling visual information than  
1219 enforcing a fixed token budget.  
1220

## 1221 F.6 COMPARISON WITH LONG VIDEO COMPRESSION METHODS

1222 We further compare FrameOracle with memory-based compression methods designed for long video  
1223 understanding. Unlike frame-selection approaches, methods such as MovieChat (Song et al., 2024),  
1224 MovieChat+ (Song et al., 2025), and ReWind (Diko et al., 2025) process video streams sequentially,  
1225 maintaining a learnable or fixed-size memory buffer that compresses historical frame features  
1226 to control context length. For a fair comparison, we reproduce MovieChat using the same backbone  
1227 as FrameOracle (LLaVA-OneVision). Following the official implementation, the reproduced  
1228 MovieChat processes up to 512 input frames, compressing them into a maximum of 64 frames for  
1229 the downstream VLM. We use the 64-frame version of FrameOracle for this comparison.  
12301231 Table 16 summarizes the results on the MovieChat-1K benchmark and other standard long-video  
1232 benchmarks. For reference, we also report the originally published numbers for MovieChat,  
1233 MovieChat+, and ReWind. On MovieChat-1K, FrameOracle achieves 69.6% accuracy, showing  
1234 that adaptive keyframe selection can match or surpass dense-frame baselines while using far fewer  
1235 frames. On long-video benchmarks such as LongVideoBench, VideoMME, and EgoSchema, Frame-  
1236

1242 Table 15: Comparison of information budgeting strategies: Frame-level (FrameOracle) vs. Token-  
1243 level (B-VLLM (Lu et al., 2025)).  
1244

1245 <b>Model</b>	1246 <b>Information</b>	1247 <b>Perception</b>	1248 <b>VideoMME</b>	1249 <b>EgoSchema</b>
1246 VideoLLaMA2+B-VLLM	1fps → 512 tokens	48.0	44.4	44.3
1247 VideoLLaMA2+FrameOracle	64 → 12.9 frames	<b>53.4</b>	<b>54.1</b>	<b>51.8</b>
1248 B-VLLM	1fps → 512 tokens	52.1	53.5	51.9
1249 LLaVA-Video+FrameOracle	64 → 12.9 frames	<b>65.1</b>	<b>61.6</b>	<b>55.2</b>

1251 Table 16: **Comparison with long video compression methods.** Note that reference methods do  
1252 not report results on newer benchmarks (indicated by -). Best performance of reference methods is  
1253 indicated by underline.  
1254

1255 <b>Model</b>	1256 <b>Frame</b>	1257 <b>MovieChat-1K</b>		1258 <b>LVB</b>	1259 <b>VideoMME</b>	1260 <b>EgoSchema</b>
		1258 <b>Acc.</b>	1259 <b>Score</b>			
<i>(1) Reference Methods</i>						
1258 MovieChat (Song et al., 2024)	1259 2048	1260 62.3	3.81	-	-	-
1258 MovieChat+ (Song et al., 2025)	1259 2048	1260 71.2	3.51	-	-	-
1258 ReWind (Diko et al., 2025)	1259 548	1260 <u>80.6</u>	<u>4.46</u>	-	-	-
<i>(2) Controlled Comparison (Backbone: LLaVA-OneVision)</i>						
1262 + MovieChat	1263 512 → 64	1264 67.1	3.44	44.2	45.6	57.8
1262 + FrameOracle (Ours)	1263 <b>64 → 15.6</b>	1264 <b>69.6</b>	<b>3.82</b>	<b>56.5</b>	<b>58.1</b>	<b>63.4</b>

1265 Oracle consistently outperforms compression-based methods, improving accuracy by up to +12.3%  
1266 on LongVideoBench. These results indicate that adaptively selecting a small set of semantically  
1267 rich keyframes provides stronger supervision and better generalization than compressing long frame  
1268 sequences into fixed tokens or memory buffers.  
12691270  
1271 

## G ADDITIONAL BENCHMARKS DETAILS

1272 Table 17 summarizes the evaluation prompts for each benchmark used in our experiments, most of  
1273 which are adapted from LMMs-Eval.  
12741275 Table 17: Prompts specifying the response format used for each evaluation benchmark.  
1276

1278 <b>Benchmark</b>	1279 <b>Response formatting prompts</b>
1280 MLVU	1281 –
1281 Video-MME	1282 Answer with the option’s letter from the given choices directly.
1282 EgoSchema	1283 Answer with the option’s letter from the given choices directly.
1283 NExTQA	1284 –
1284 Perception	1285 Answer with the option’s letter from the given choices directly.
1285 LongVideoBench	1286 Answer with the option’s letter from the given choices directly.

1287  
1288 

## H FRAMEORACLE-41K EXAMPLES

1289 Figure 7 shows three examples from the FrameOracle-41K dataset. Each example demonstrates the  
1290 number of selected keyframes, the associated question, the ground-truth answer, and the question  
1291 type. We also provide indices for the selected keyframes within the 64 uniformly sampled frames  
1292 used during preprocessing, indicating their relative positions along the video timeline. These examples  
1293 highlight the diversity of reasoning types in FrameOracle-41K, such as causal reasoning and  
1294 fine-grained action understanding, and illustrate that the annotations focus on semantically informative  
1295 moments rather than evenly spaced frames.

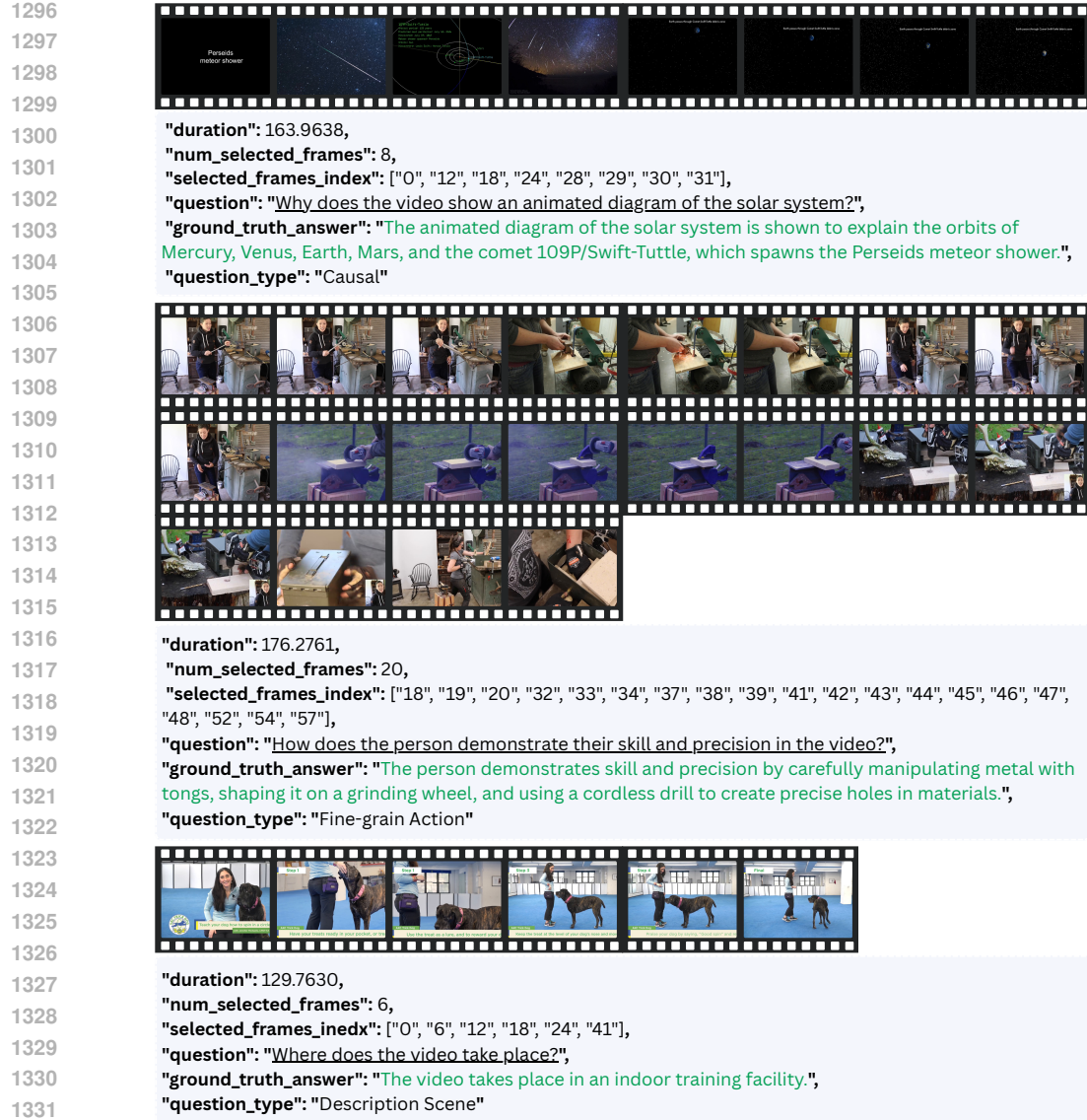


Figure 7: **Examples from the FrameOracle-41K dataset.** Each example shows the number of selected keyframes, question, ground-truth answer, question type, and the indices of the selected keyframes.

## I QUALITATIVE EXAMPLES

As shown in Figure 8, FrameOracle can achieve correct answers using far fewer frames than uniform sampling. In the illustrated examples, our selector retains only 2–4 frames out of the original 16 inputs, yet these frames provide sufficient evidence to answer the questions accurately. This highlights that many uniformly sampled frames are redundant and that FrameOracle effectively filters them without sacrificing accuracy.

Figure 9 presents cases related to RQ1 (Section 5.2). Providing all 16 uniformly sampled frames can introduce irrelevant or distracting content, leading the VLM to produce incorrect answers. In contrast, FrameOracle selects a smaller, query-focused subset, allowing the model to concentrate on relevant evidence and answer correctly. These examples illustrate that more frames do not necessarily improve performance, and adaptive selection of fewer, informative frames enhances understanding.

1350

1351

1352

*Question:* What did the man in the front do when the man at the back after the man at the back picked up the spoon?

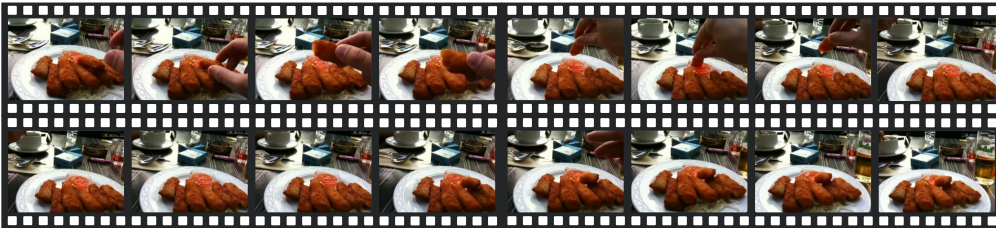
- A. take the bowl
- B. places pan back on stove
- C. dip food into sauce**
- D. does hand gesture toward the tiger
- E. help to season other chickens

1356

1357

#### Uniform Sampling (Qwen2.5-VL: C)

1359



1360

1361

1362

1363

1364

1365

1366

1367

#### FrameOracle (Qwen2.5-VL: C)

1368

1369



1370

1371

1372

1373

1374

1375

1376

*Question:* Why is the man wearing slippers sitting at the top of the rock at the start of the video?

- A. take photo from angle
- B. sunbathing
- C. preparing for a performance
- D. to pose for the camera
- E. waiting to jump in water**

1377

1378

1379

1380

1381

1382

#### Uniform Sampling (Qwen2.5-VL: E)

1383

1384



1385

1386

1387

1388

1389

1390

1391

1392

1393

#### FrameOracle (Qwen2.5-VL: E)

1394

1395

1396

1397

1398

1399

1400

1401

1402

1403



Figure 8: **Qualitative examples.** FrameOracle answers correctly while using only a few frames (2 to 4 out of 16), compared to uniform sampling, which relies on the full input.

1404

1405

*Question:* What seems to be the main purpose of the video? What actions did c perform to achieve this purpose?

1406

A: The main objective of this instructional video is to effectively demonstrate how to easily tie your hair back.

1407

B: The main purpose of the video is to show how to open a jar.

1408

C: The primary objective of the video presentation is to demonstrate the most effective methods for properly cleaning your windows.

1409

**D: The main purpose of the video is to show how to use a resistance band to exercise your arms and upper body.**

1410

E: The primary objective of this video presentation is to effectively demonstrate the proper way to engage in a fun tug-of-war match with your canine companion.

1411

1412

**Uniform Sampling (Qwen2.5-VL: A)**

1413



1414

1415

1416

1417

1418

1419

1420

1421

**FrameOracle (Qwen2.5-VL: D)**

1422

1423

1424

1425

1426

1427

1428

1429

1430

1431

*Question:* From the sequence of actions, identify a turning point or moment where c's focus shifts to a different task. explain why you believe this is the most significant part of the video.

1432

**A: The turning point is when c unfastens the hub axle.**

1433

B: The crucial turning point occurs when character c picks up the screwdriver from the table.

1434

C: The pivotal turning point occurs when character c decides to put on the gloves.

1435

D: The turning point is when c removes the tire.

1436

E: The critical turning point occurs when character c successfully patches the hole, fixing it.

1437

1438

**Uniform Sampling (Qwen2.5-VL: B)**

1439

1440

1441

1442

1443

1444

1445

1446

1447

1448

1449

1450

1451

1452

1453

1454

1455

1456

**Figure 9: Qualitative examples for RQ1.** Using all 16 uniformly sampled frames can produce incorrect answers, whereas FrameOracle answers correctly by selecting only the relevant subset.